

NOLAN ROSS WHEILDON, B.Sc.

Lung Extracellular Matrix Effects on Fibroblast/Myofibroblast Phenotype

EXPERIMENTAL METHODS TO ELUCIDATE LUNG EXTRACELLULAR
MATRIX EFFECTS ON FIBROBLAST/MYOFIBROBLAST PHENOTYPE

By

NOLAN ROSS WHEILDON, B.Sc.

A Thesis Submitted to the School of Graduate Studies In Partial Fulfillment of the
Requirements For the Degree Master of Science

McMaster University

© Copyright by Nolan Ross Wheildon, November 2014

Descriptive Note

MASTER OF SCIENCE (2014)
(Medical Sciences)

McMaster University
Hamilton, Ontario

TITLE: EXPERIMENTAL METHODS TO ELUCIDATE LUNG EXTRACELLULAR
MATRIX EFFECTS ON MYOFIBROBLAST PHENOTYPE

AUTHOR: Nolan Ross Wheildon, B.Sc. (University of Guelph)

SUPERVISORS: Dr. Luke Janssen and Dr. Martin Kolb

NUMBER OF PAGES: xiv, 83

Abstract

Introduction

Idiopathic pulmonary fibrosis (IPF) is a debilitating restrictive lung disease with no curative treatments. Accumulation of lung extracellular matrix (ECM) and myofibroblasts are two hallmarks of this disease. Previous studies have demonstrated that an increase in lung ECM in the formation of scar tissue promotes further myofibroblast accumulation exacerbating IPF disease progression. Lung ECM influence on myofibroblast phenotype is not fully understood. Methods to elucidate lung ECM effects on myofibroblast phenotype were developed in this thesis.

Aim

This study sought to determine whether lung ECM could modulate fibroblast/myofibroblast phenotype.

Methods

Histological and western blot analyses were used to evaluate lung ECM isolation through manual decellularization of whole rat lungs with sodium deoxycholate (SDC). To evaluate the effects decellularization has on lung ECM, histological analyses were conducted to compare sodium dodecyl sulfate (SDS) and SDC ability to retain collagen and elastic fibers following decellularization. Histological examination of drop-wise and whole lung reseeding techniques of decellularized lung ECM were assessed. To further mimic *in vivo* conditions, a novel lung bioreactor incorporating physiological lung respiration and vascular perfusion was developed. The effects of stiff cell culture plastic on alpha smooth muscle actin (α -SMA) phenotype of control and IPF-derived

myofibroblasts were evaluated. Western blot, immunohistochemistry, immunocytochemistry, and immunofluorescent analyses were used to evaluate whether normal lung ECM could reverse the α -SMA positive phenotype of lung myofibroblasts.

Results

Manual decellularization with SDC was effective at decellularizing whole rat lung. Histological examination showed that SDC was more effective at retaining collagen and elastic fibers than SDS following decellularization. Whole lung reseeding technique was far superior compared to the drop-wise technique at consistently reseeding lung ECM. Lung bioreactor maintained A549 cells within decellularized whole lung for 3 days. Furthermore, normal lung ECM was capable of reversing α -SMA positive phenotype of both control and IPF-derived myofibroblasts.

Conclusions

Methods developed in this thesis advances the understanding of decellularization and reseeding techniques required to study lung ECM on cell phenotype. Interestingly, and contrary to previous work, it appears that α -SMA phenotype of myofibroblasts was reversible when cultured on normal lung ECM.

Acknowledgements

I would like to sincerely thank my supervisors, Dr. Luke Janssen and Dr. Martin Kolb, for providing me an opportunity to complete my Master's degree. Over the past two years, Luke has supported and guided me through many academic and personal challenges. I would also like to thank Martin for his continued guidance through the technical and academic challenges that occurred throughout this project. I would like to thank both of you for your guidance and leadership, which helped me grow as an academic and as a person and I will be forever indebted to both of you.

I am very grateful of Dr. Kjetil Ask for being part of my supervisory committee. Your advice and expertise was critical for the success of this project.

I would like to thank all the members of both Martin's and Luke's labs. I would also like to thank my knowledgeable and invaluable post-doctoral colleagues: Dr. Subehndu Mukherjee, Dr. Chiko Shimbori, and Dr. Pierre-Simon Bellaye. Thank you to Subhendu for helping with the calcium experiments and being supportive throughout my project. Thank you to Chiko for helping with animal experiments, western blotting, and countless other techniques; this project would not have been as successful if you were not involved. Last but not least, thank you to Pierre who brought an infinite amount of knowledge and technical skills to this project, and for helping me through some of the most difficult aspects of this project.

I would like to thank my mother, brother, partner, and family members who have supported me throughout my studies. To my partner, and best friend, thank you for listening and encouraging me throughout this project. I would not have been able to

complete this project without you. To my mother, I am forever thankful for your brilliance, encouragement, and sacrifices that have allowed me to have a wonderful personal and academic life.

Table of Contents

Descriptive Notei

Abstract..... ii

Acknowledgementsiv

Table of Contentsvi

List of Figures.....x

List of Abbreviations xii

Declaration of Academic Achievementxiv

Chapter 1: Introduction 1

1.1 Statement of problem 1

1.2 Characteristics and origins of myofibroblasts in pulmonary fibrosis 2

 1.2.1 Characteristics..... 2

 1.2.2 Origins..... 3

 1.2.2.1 Epithelial Cells..... 5

 1.2.2.2 Fibrocytes..... 5

 1.2.2.3 Pericytes 6

 1.2.2.4 Endothelial Cells..... 7

 1.2.2.5 Mesothelial Cells 7

1.3 Components of lung ECM and their role in regulating fibroblast phenotype 8

 1.3.1 Collagen 9

1.3.2 Fibronectin	10
1.3.3 Glycosaminoglycans and Proteoglycans.....	11
1.3.4 TGF- β	13
1.3.5 Stiffness induced fibroblast differentiation.....	14
<i>1.4 Cell culture models to elucidate lung ECM effects on fibroblast and myofibroblast phenotype</i>	<i>15</i>
1.4.1 2D plastic cell culture system	15
1.4.2 2D silicone soft and stiff culture system.....	16
1.4.3 3D collagen gel cell culture system	17
1.4.4 Native lung ECM as a 3D cell culture system	17
<i>1.5 Purpose of study and hypothesis.....</i>	<i>18</i>
Chapter 2: Materials and Methods	19
<i>2.1 Lung Explant.....</i>	<i>19</i>
<i>2.2 Soft plate cell culture</i>	<i>19</i>
<i>2.3 Animal Experiments</i>	<i>19</i>
<i>2.4 Lung slice elastance.....</i>	<i>20</i>
<i>2.5 Western Blot analysis.....</i>	<i>20</i>
<i>2.6 Histology.....</i>	<i>21</i>
<i>2.7 Immunohistochemistry, Immunocytochemistry and immunofluorescence.....</i>	<i>21</i>
<i>2.8 Statistics</i>	<i>22</i>
Chapter 3: Development of Methods to Elucidate Lung ECM Effects on Fibroblast/Myofibroblast Phenotype	23

<i>3.1 Aims</i>	23
<i>3.2 Decellularization and Reseeding of Lung Slices</i>	23
3.2.1 Background	23
3.2.2 Decellularization Protocol	23
3.2.3 Reseeding Protocol	24
3.2.4 Results	25
3.2.5 Discussion	27
<i>3.3 Whole Rat Lung Decellularization and Reseeding</i>	28
3.3.1 Background	28
3.3.2 Decellularization Protocol	28
3.3.3 Reseeding Protocol	30
3.3.4 Results	31
3.3.5 Discussion	34
<i>3.4 Rapid whole lung decellularization</i>	35
3.4.1 Background	35
3.4.2 Decellularization Protocol	37
3.4.3 Preliminary Results	39
3.4.4 Discussion	41
<i>3.5 Lung Bioreactor Design and Culture</i>	43
3.5.1 Background	43
3.5.2 Design	44
3.5.3 Lung bioreactor culture	45

3.5.4 Preliminary Results	45
3.5.5 Discussion	46
<i>3.6 Examination of lung ECM's effects on myofibroblast calcium handling</i>	<i>47</i>
3.6.1 Background	47
3.6.2 Methods.....	48
3.6.3 Discussion	51
Chapter 4: Elucidating Lung ECM Effects on Myofibroblast Phenotype	52
<i>4.1 Aims.....</i>	<i>52</i>
<i>4.2 Background.....</i>	<i>52</i>
<i>4.3 Results</i>	<i>53</i>
<i>4.4 Discussion.....</i>	<i>61</i>
<i>4.5 Limitations and Future Directions.....</i>	<i>64</i>
References.....	67

List of Figures

Figure	Description	Page
1	Origins of myofibroblast in pulmonary fibrosis.....	4
2	Young’s modulus of tissues	14
3	H&E staining of decellularized lung slices.....	25
4	H&E staining of reseeded decellularized lung slices	26
5	Macroscopic, histologic, and western blot analyses of normal freshly fixed, PBS washed, and decellularized whole rat lungs	31
6	Comparison of drop-wise and whole lung reseeded techniques.....	32
7	Timeline of fibroblast migration out of agarose onto decellularized whole rat lung ECM	33
8	Schematic of rapid whole lung decellularization set-up	37
9	Histological comparison of various decellularizing agents utilizing rapid decellularization technique.....	39
10	Histological comparison of decellularizing agent’s effects on retaining lung ECM following rapid decellularization.....	40
11	Schematic of lung bioreactor set-up.....	44
12	H&E of A549 cells cultured within bioreactor.	45
13	Representation of IPF-derived myofibroblast calcium handling cultured on glass vs. normal lung ECM	49
14	Quantification of normal lung ECM’s effect on IPF-derived myofibroblast calcium handling	50

15	Evaluation of lung slice elastance	54
16	Comparison of control and IPF-derived myofibroblast α -SMA expression when explanted and cultured on plastic	55
17	Immunofluorescence of control and IPF-derived myofibroblast α -SMA expression cultured on plastic	56
18	Comparison of control and IPF-derived myofibroblast α -SMA expression following culture on plastic vs. normal lung ECM through western blot analysis	57
19	Comparison of control and IPF-derived myofibroblast α -SMA expression following culture on plastic vs. normal lung ECM through immunocytochemistry and immunohistochemistry	58
20	Evaluation of stiff vs. soft cell culture plate effect on control myofibroblast α -SMA expression.....	59
21	Evaluation of normal lung ECM's effect on myofibroblast apoptosis	60

List of Abbreviations

3-[(3-Cholamidopropyl)dimethylammonio]-1-propanesulfonate-CHAPS

Acetylated glutamic acid (3x)-aspartic acid-AcEEED

Alpha smooth muscle actin- α -SMA

American Thoracic Society-ATS

C-C chemokine receptor

C-X-C chemokine receptor

Deoxyribonuclease I-DNase I

Double deionized water-ddH₂O

Elastin Van Gieson-EVG

Endothelial-to-mesenchymal-EndoMT

Epithelial to mesenchymal-EMT

Ethylenediaminetetraacetic acid-EDTA

European Respiratory Society-ERS

Extracellular Matrix-ECM

Glyceraldehyde 3-phosphate dehydrogenase -GAPDH

Glycosaminoglycans-GAGs

Hematoxylin and Eosin-H&E

Idiopathic pulmonary fibrosis-IPF

Japanese Respiratory Society-JRS

Phosphate Buffered Saline-PBS

Picro Sirius Red-PSR

Platelet-derived growth factor-PDGF

Sodium chloride-NaCl

Sodium deoxycholate-SDC

Sodium dodecyl sulfate-SDS

The extra type III domain A-EDA

The Latin American Thoracic Association-ALAT

The mothers against decapentaplegic-SMAD

Transforming growth factor beta-TGF- β

Declaration of Academic Achievement

I personally accomplished all the research necessary to generate figures 1-19 and 21. For figure 20, I helped design the experiment with Pierre-Simon Bellaye, but Pierre carried out the experiment.

Chapter 1: Introduction

1.1 Statement of problem

IPF is characterized as a restrictive lung disease causing impairment in lung expansion and gas exchange. This restriction in gas exchange is due to an increase in parenchymal scarring and thickening of the ECM that surrounds the alveoli (ATS/ERS consensus 2002). The factors that cause the disease remain elusive making the treatment of the disease more difficult. The median age of IPF onset ranges from 60-70 years of age (Poletti et al. 2013). Prevalence of IPF in United States was estimated to be 42.7 per 100,000 with an incidence rate of 16.3 per 100,000 deaths per year (Raghu et al. 2006). Additionally, depending on initial stage of diagnosis, the median survival of IPF patients range from 3-5 years (Hubbard et al. 1997).

Furthermore, the treatment options for patients diagnosed with IPF remain limited. Initial drugs to treat IPF included: corticosteroids, cyclophosphamide, azathioprine, and N-acetylcysteine. An official ATS/ERS/JRS/ALAT statement recommended that these drugs should not be used to treat IPF patients due to a lack of evidence-based improvement in disease. Pirfenidone, an anti-fibrotic and anti-inflammatory drug, is an approved treatment of IPF in Canada, Japan, and Europe. Recently published phase 3 clinical trials evaluating Nintedanib, an inhibitor of multiple tyrosine kinases, revealed that this drug was effective in reducing lung function decline and exacerbations in IPF patients compared to placebo (Richeldi et al. 2014). Nevertheless, lung transplantation remains the only treatment option that can restore respiration for IPF patients; however, the shortage of possible organ donors limits this treatment option (Raghu et al. 2011).

Consequently, there is a need for further understanding of the underlying mechanisms contributing to the development and progression of IPF in order to develop more effective treatment options. Two key components contributing to the development and progression of IPF are accumulation of extracellular matrix in the formation of scar tissue and the persistence of myofibroblasts. Myofibroblasts are key effector cells in IPF since they are responsible for the synthesis and deposition of ECM. The effects that lung ECM has on fibroblast/myofibroblast phenotype has not yet been fully elucidated. To fully elucidate this relationship, knowledge of myofibroblast characteristics and origins and the components of lung ECM that may impact fibroblast to myofibroblast differentiation need to be explored.

1.2 Characteristics and origins of myofibroblasts in pulmonary fibrosis

1.2.1 Characteristics

The myofibroblast has long been thought to be a key player in driving the pathogenesis of IPF (King et al. 2001). Under normal conditions, fibroblasts express little cell-to-cell and cell-to-matrix interactions, and produce far less ECM in comparison to the myofibroblast (Tomasek et al. 2002). Following tissue injury, fibroblasts differentiate into myofibroblasts, which are distinguished from fibroblasts through the appearance of spindle morphology. Additionally myofibroblasts, possess stress fibers that have increased contractile properties due to an increase in α -SMA expression (Schürch et al. 1998, Hinz et al. 2001). The N-terminal amino acid sequence acetylated glutamic acid (3x)-aspartic acid sequence (AcEEED) found in α -SMA has been thought to be the key contributor to its ability to increase myofibroblast contractility. To test this hypothesis,

Hinz et al. (2002) delivered a fusion protein containing the AcEEED binding domain into lung myofibroblasts resulting in reduced cell tension/contraction.

During normal wound healing, fibroblast to myofibroblast differentiation is required for proper wound healing and contraction of the wound. The main difference between normal wound healing and the runaway scar formation in IPF is that myofibroblasts will be eliminated through apoptosis following resolution of wound healing. Myofibroblasts have been shown to have increased resistance to apoptosis during normal wound healing, as demonstrated through *in situ* end labeling of fragmented DNA. However, following the resolution of normal wound healing, these myofibroblasts disappear through apoptosis (Desmoulière et al. 1995). On the other hand, IPF myofibroblasts have been shown to acquire continued resistance to apoptosis (Maher et al. 2010).

1.2.2 Origins

Myofibroblasts arise during normal wound repair to aid in the closure of wounds. Until the last decade, the prevalent hypothesis was that myofibroblasts arose specifically from undifferentiated fibroblasts. An early study conducted by Zhang et al. (1994) demonstrated that myofibroblasts were responsible for increased collagen gene expression in bleomycin induced pulmonary fibrosis and that the sources of these myofibroblasts were from perivascular and peribronchiolar adventitial fibroblasts. However, more recent studies have demonstrated that resident fibroblasts, pericytes, epithelial cells, endothelial cells, fibrocytes, and mesothelial cells may all contribute to the accumulation of myofibroblasts in IPF (Figure 1; Abe et al. 2001, Frid et al. 2002,

Kalluri et al. 2003, Phillips et al. 2004, Willis et al. 2005, Kim et al. 2006, Decolonne et al. 2007, Moeller et al. 2009, Hashimoto et al. 2010, Rock et al. 2011, Hutchison et al. 2013).

Cell Origins of Pulmonary Myofibroblast

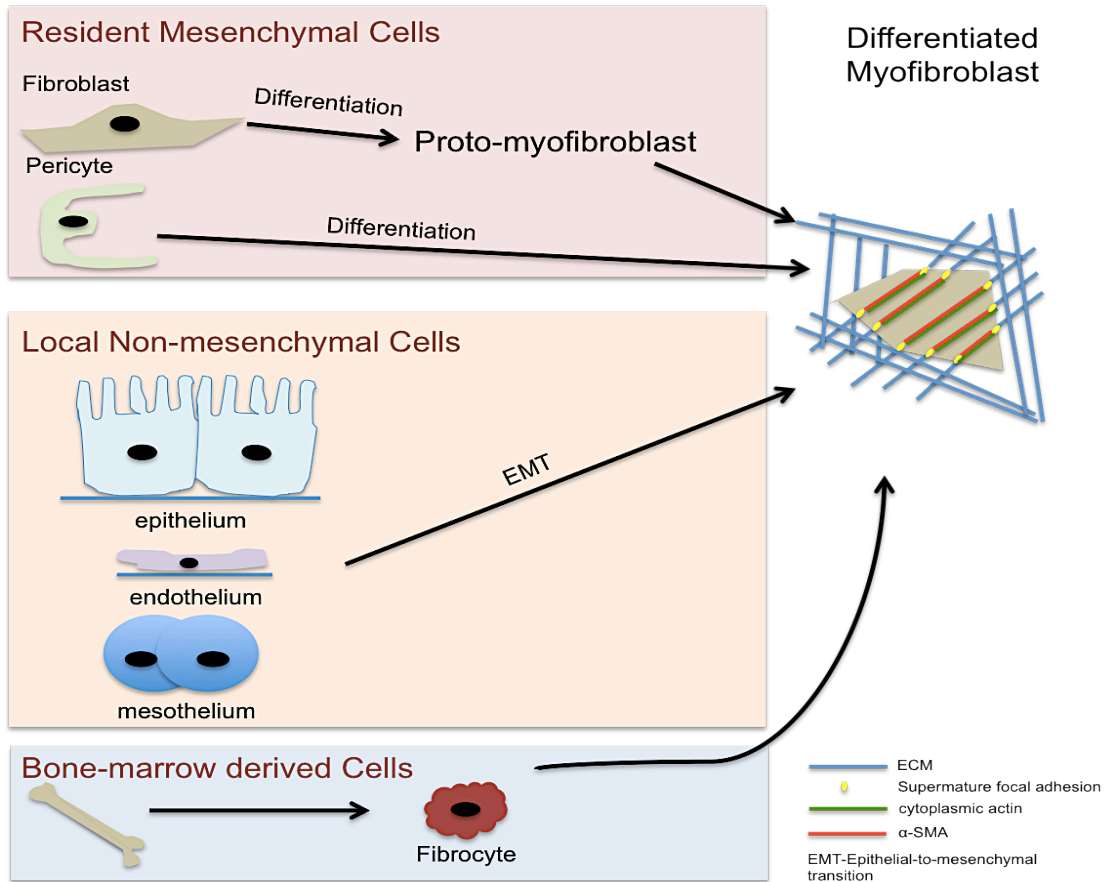


Figure 1-Origins of myofibroblast in pulmonary fibrosis

Adopted from Hinz et al. (2007) represents sources of myofibroblasts in IPF. Light pink box represents mesenchymal cells in the lung; beige box represents non-mesenchymal cells in the lung; light blue box represents bone marrow derived cells. The differentiated myofibroblast is illustrated with the typical stress fibers containing α -SMA connected to ECM through focal adhesions.

1.2.2.1 Epithelial Cells

The transition of epithelial to mesenchymal (EMT) cells has been widely accepted as a source of myofibroblasts. EMT occurs when epithelial cells are exposed to transforming growth factor beta (TGF- β) leading to the activation of the profibrotic molecules against decapentaplegic (SMAD) 2,3,4 proteins. These SMAD proteins induce transcription factors like Slug, Snail, and β -catenin promoting a cellular environment of E-cadherin disassembly, cytoskeletal rearrangement, increased α -SMA expression, and increased cellular motility (Kalluri et al. 2003, Zavadil et al. 2005). The Rho-kinase pathway also leads to EMT through E-cadherin down regulation and cytoskeleton rearrangement (Masszi et al. 2003). Conversely a study evaluating EMT transition using a bleomycin induced pulmonary fibrosis model failed to demonstrate that epithelial cells were a source of myofibroblasts (Barth et al. 2005, Rock et al. 2011). Although this study did mention that their *in vivo* analysis may have been conducted too late to detect EMT as a source of myofibroblasts.

1.2.2.2 Fibrocytes

Fibrocytes are mesenchymal precursor cells derived from the bone marrow. They possess a distinctive phenotype (collagen +/vimentin +/CD34 +), and are characterized by their rapid transfer from the blood through areas of damaged connective tissue. They also express many chemokine receptors such as C-C chemokine receptor 3 (CCR), CCR5, CCR7, and C-X-C chemokine receptor R4 that are responsible for their recruitment at inflammatory lesions (Abe et al. 2001). Cells that express specific markers of fibrocytes were found in the lung parenchyma of IPF patients, potentially showing a process of

migration and "homing" of these cells contributing to an increase in fibroblasts/myofibroblasts in the microenvironment of the fibrotic lung (Andersson-Sjoland et al. 2008). Philips et al. (2004) conducted a study demonstrating that in response to bleomycin-induced pulmonary fibrosis, fibrocytes would traffic to the lungs at the height of collagen deposition. Fibrocytes were shown to be elevated in the blood of IPF patients and that there was a further increase during exacerbations highlighting fibrocytes role as a prognostic indicator in IPF (Moeller et al. 2009). However, the validity of fibrocytes as a source of myofibroblasts remains debatable. Yokota et al.'s (2006) study concluded that bone marrow derived cells were unlikely to be a source of myofibroblasts. This study transplanted green fluorescent labeled α -SMA bone marrow to a mouse that was subsequently administered bleomycin to induce pulmonary fibrosis, which resulted in no green fluorescent labeled α -SMA lung myofibroblasts.

1.2.2.3 Pericytes

Present theory shifted focus away from epithelial cells as being the main source of myofibroblasts to stromal and pericyte cells from surrounding vasculature as a major source of myofibroblasts within fibrotic disease. This was demonstrated when Rock et al. (2011) showed in a bleomycin model of pulmonary fibrosis pericytes, not type II alveolar epithelial cells, were the dominant cell type that contributed to α -SMA expressing myofibroblasts. This observation was made previously in a model of kidney fibrosis, where it was also observed that pericytes and not epithelial cells contributed to subsequent myofibroblast population (Humphreys et al. 2010).

1.2.2.4 Endothelial Cells

Endothelial cells as a source of myofibroblasts in fibrosis occurs through endothelial-to-mesenchymal (EndoMT) pathway similar to EMT where endothelial cells lose their endothelial phenotype (e.g. CD31) and adopt α -SMA positive mesenchymal phenotype. An early study demonstrated that endothelial cells could transdifferentiate through EndoMT to gain a phenotype resembling smooth muscle cells noted by expression of α -SMA. This process was TGF- β and cell-to-cell contact dependent (Frid et al. 2002), similar to what may occur in IPF. Additionally, Hashimoto et al. (2010) demonstrated that labelled endothelial cells in transgenic mice gave rise to collagen I and α -SMA positive fibroblasts in bleomycin induced fibrotic lungs.

1.2.2.5 Mesothelial Cells

Decologne et al. (2007) induced pleural fibrosis through administration of TGF- β loaded adenovirus into the pleural space of a rat lung, which induced pleural fibrosis eventually manifesting into parenchymal fibrosis. They demonstrated that the mesothelial cells of the pleura transdifferentiated into myofibroblasts in the pleural area of the lung and that this cell type could migrate toward the parenchyma leading to pulmonary fibrosis. The transdifferentiation of mesothelial cells to mesenchymal has been attributed to the mesothelial-fibroblastoid transformation. This transdifferentiation has been demonstrated in peritoneal fibrosis where overexpression of TGF- β 1 contributed to mesothelial cells adopting a α -SMA positive mesenchymal phenotype (Margetts et al. 2005).

1.3 Components of lung ECM and their role in regulating fibroblast phenotype

One of the major functions of the ECM is to support and maintain structural integrity for cells, tissues, and organs. Additionally, the ECM's structure and stiffness plays an important role in modifying cellular activities, such as: proliferation, migration, differentiation, adhesion, and apoptosis (Hynes 2009). Furthermore, following tissue injury, the ECM releases stored growth factors and cytokines, along with matrikines, that help drive wound healing and tissue repair. Finally, ECM provides structural cues for proper branching morphogenesis.

Lung ECM contains many proteins and polysaccharides most notably: collagen I, III, IV, V; elastins; laminins; glycosaminoglycans; and proteoglycans. Together these components form a heterogeneous meshwork in terms of stiffness and softness. In IPF lungs, the ECM stiffness is increased due to buildup of scar tissue, which ultimately contributes to the regression of lung function. It has been shown that collagen type I synthesis is increased in fibrotic rat lungs following bleomycin treatment (Van Hoozen et al. 2000). Booth et al. (2012) conducted a detailed analysis of normal and fibrotic lung ECM composition through mass spectrometry, which revealed increased collagen I and glycosaminoglycan deposition in IPF lungs. Furthermore, Venkatesan et al. (2011) showed changes in the distribution of glycoproteins and glycosaminoglycans in fibrotic matrix compared to normal matrix.

Fibroblast to myofibroblast differentiation requires crucial biochemical and biomechanical events to occur that are influenced by the ECM. First, there needs to be release of active TGF- β . The expression or overexpression of certain ECM components

like collagen I need to occur as well. Finally, and maybe most importantly for the propagation of myofibroblast accumulation in IPF, increased extracellular stress/increased stiffness of ECM has to occur (Tomasek et al. 2002).

1.3.1 Collagen

The bulk of lung ECM consists of collagen I and III for tensile strength, and elastin for recoil of the lungs (Rocco et al. 2001, Cavalcante et al. 2005). On the other hand, collagen IV is a major stabilizing component of the parenchymal basement membrane (Pöschl et al. 2004). Recently, it was shown that serum samples from IPF patients had elevated collagen IV alpha 1 and 3 chains via degradation of the basement membrane by matrix metalloproteinase-12 (Sand et al. 2013). It has been shown that during the development of IPF there is an increase in collagen synthesis, especially scar forming collagen type I, and deposition highlighting collagen's role in IPF (Van Hoozen et al. 2000, Kolb et al. 2001). Moreover, collagen V was shown to have increased deposition in bleomycin induced pulmonary fibrosis (Blaauboer et al. 2014). Additionally, intravenous pretreatment of collagen V before bleomycin administration resulted in attenuation of lung fibrosis that was associated with a reduction in interleukin-6 and 17 highlighting collagen V role in initiation of pulmonary fibrosis (Braun et al. 2010).

Collagens possess inter and intrachain crosslinking due to their ability to align in a staggered head-to-tail formation. This allows crosslinking between aldehyde groups on aligned lysine or hydroxylysine amino acids (Reiser et al. 1992) that are facilitated by the lysyl oxidase enzyme (Kagan et al. 1991). Crosslinking of collagen can occur with a

number of other ECM components like fibronectin and glycosaminoglycans bound to proteoglycans (Dzamba et al. 1993, San Antonio et al. 1994). Prolyl-4-hydroxylase and transglutaminase 2 are two other crosslinking enzymes of interest in prevention of fibrosis. A previous study of liver fibrosis showed that the administration of an inhibitor of prolyl-4-hydroxylase diminished the fibrotic response (Bickel et al. 1998). Furthermore, mice lacking transglutaminase 2 experienced a reduction in fibrosis when challenged with bleomycin as demonstrated through a decrease in collagen content (Olsen et al. 2011). It appears that increased cross-linking between ECM components may provide therapeutic targets for treatment of IPF.

1.3.2 Fibronectin

Fibronectins have been implicated in the progression of IPF; they are typically found in uncharacteristically high amounts preceding areas of fibrotic tissue (Hernnäs et al. 1992). The extra type III domain A (EDA) containing fibronectin has been studied in the context of fibrosis since it contributes to wound healing and fibroblast differentiation (Serini et al. 1998, Muro et al. 2003). It has been shown that TGF- β 1 induces an increase in EDA-fibronectin expression (Vaughan et al. 2000) that is necessary for the differentiation of fibroblast to myofibroblast (Serini et al. 1998). Mice lacking EDA resulted in the failure to phosphorylate SMAD2 protein in response bleomycin administration suggesting that *in vivo* fibronectin EDA is required for full activation of the TGF- β pathway. This lack of TGF- β activation was evident through reduction in fibroblast to myofibroblast differentiation noted by a reduction in α -SMA expression in EDA knockout mice compared to wild type mice in a bleomycin model of lung fibrosis

(Muro et al. 2008). This work suggested EDA-fibronectin was required for cleavage of TGF- β from its latent binding protein.

More recent work shows that EDA-fibronectin ability to induce fibroblast to myofibroblast differentiation depends on $\alpha_4\beta_7$ integrin. This was illustrated when an anti- $\alpha_4\beta_7$ integrin antibody was administered to block EDA-fibronectin binding resulted in a reduction in fibroblast to myofibroblast differentiation. It appears that EDA-fibronectin ability to differentiate fibroblast to myofibroblast through $\alpha_4\beta_7$ integrin promotes phosphorylation of focal adhesion kinase and increased phosphorylation of mitogen-activated protein kinase, which regulates cell differentiation (Kohan et al. 2010).

1.3.3 Glycosaminoglycans and Proteoglycans

Glycosaminoglycans (GAGs) are able to attach to a core protein to form a proteoglycan complex, which helps to stabilize the lung ECM during compression while keeping the ECM hydrated (Papakonstantinou et al. 2009). The composition of proteoglycans has a defining role in lung elasticity and alveolar stability through stabilization of the collagen and elastic network during respiration (Cavalcante et al. 2005). Two distinct types of GAGs are found in the lung, sulphated and non-sulphated GAGs. Sulphated GAGs consist of: heparan sulfate/heparin, chondroitin/dermatan sulfate, keratan sulfate. Hyaluronic acid represents the non-sulfated GAG in the lung (Souza-Fernandes et al. 2006).

The lung has distinguishable proteoglycan complexes: versican-a chondroitin sulfated proteoglycan, perlecan and glypican-a heparan sulfated proteoglycans, syndecan-a chondroitin or heparan sulfated proteoglycan, and decorin-a dermatan sulfated

proteoglycan. Additionally, there are small leucine rich repeat proteoglycans called biglycan and fibromodulin. Biglycan binds TGF- β influencing matrix assembly (Ruoslahti et al. 1991) and fibromodulin also binds to TGF- β influencing collagen fiber formation (Hedbom et al. 1989, Iozzo et al. 1998).

Versican binds hyaluronic acid and surrounds lung fibroblasts within the parenchyma regulating differentiation of mesenchymal cells and has been hypothesized to support wound healing (Iozzo et al. 1996). Perlecan interacts with collagen IV along the basement membrane to constrain the movement of macromolecules/cells among tissue compartments. Additionally, perlecan has been shown to control the interaction of the basic fibroblast growth factor 2 through its heparan sulfate side chains impacting the initiation of wound healing (Yurchenco et al. 1990, Zhou et al. 2004). Syndecan participates in fibroblast's matrix assembly and increased proliferation (syndecan-2); cell-matrix attachment and initiation of wound healing (syndecan-4); and wound healing through its interactions with heparin binding growth factors and extracellular proteins like fibronectin and laminin (Klass et al., 2000, Tumova et al. 2000, Echtermeyer et al. 2001, Villena et al. 2003, Midwood et al. 2004). Decorin acts to modulate tissue remodeling through alteration of collagen fibril formation. This was demonstrated in a decorin double knockout mouse where there was development of weaker, abnormal collagen fibrils modulating tissue remodeling (Reed et al. 2003). Studies have shown an overall increase in GAGs and proteoglycans synthesis and deposition during IPF (Nettelbladt et al. 1989, Venkatesan et al. 2011). With this aforementioned information in hand, it is clear GAGs and proteoglycans play a vital role in maintaining lung homeostasis.

1.3.4 TGF- β

Mammals express three different isoforms of transforming growth factor beta: TGF- β 1, TGF- β 2, and TGF- β 3. TGF- β 1 has been implicated in majority of fibrotic diseases plaguing humans (Border and Noble 1994), and overexpression of TGF- β 1 was shown to induce pulmonary fibrosis (Sime et al. 1997). TGF- β 1 is produced in a latent form that is sequestered in the lung ECM until it is cleaved into active form through separation from the latent associated peptide (Derynck et al. 1985, Wakefield et al. 1988). Physical process such as acidification, temperature changes, and oxidation can activate TGF- β 1 (Pociask et al. 2004, Sullivan et al. 2008). It has been demonstrated *in vitro* that proteases like tryptase, thrombin, elastase, and matrix metalloproteinase-2 and 9 can cleave the latent associated peptide activating TGF- β 1. *In vivo* studies demonstrate that integrins (eg. $\alpha_v\beta_6$) are responsible for activation of TGF- β 1 (Jenkins et al. 2008). Fibroblast to myofibroblast differentiation is induced by activated TGF- β 1 (Desmoulière et al. 1993, Sime et al. 1997). The inactivated form of TGF- β 1 is embedded in lung ECM, thus TGF- β activation is a crucial mechanism in which lung ECM can modulate fibroblast and myofibroblast differentiation.

1.3.5 Stiffness induced fibroblast differentiation

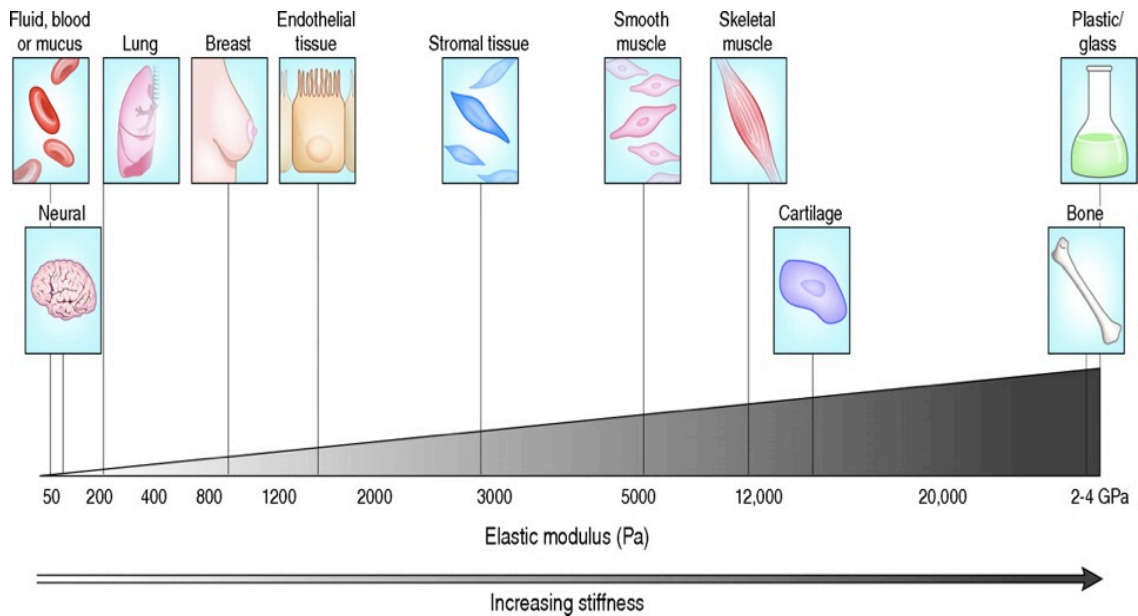


Figure 2-Young's modulus of tissues

Representation of elasticity of tissues and organs in the human body (Cox and Erler 2011). Normal lung stiffness is 0.5-1kPa and fibrotic lung ECM's stiffness varies from 6-20 kPa (Liu et al. 2010).

Recent work has demonstrated that increased lung ECM stiffness through culture on stiff traditional cell culture plates alone induces fibroblast to myofibroblast differentiation (Liu et al 2010, Balestrini et al. 2012). Promotion of this differentiation is through increased cell anchoring to ECM producing increased cellular tension, which then initiates differentiation of fibroblast to myofibroblast, noted by increased α -SMA expression. Increased anchoring promotes an increase in phosphorylation of myosin light chain kinase and focal adhesion kinase promoting a further increase in cellular tension and the formation of supermature focal adhesions (Goffin et al. 2006, Hinz et al. 2006). Overall, increased tension leads to myofibroblast differentiation and increased

myofibroblast contraction. In addition, Wipff et al. (2007) demonstrated that increased ECM stiffness promoted increased myofibroblast contraction activating TGF- β 1 through cleavage from its latent binding compared to soft ECM. They demonstrated that this mechanism was integrin mediated as well.

Further examination of specific integrins involved in activation of TGF- β 1, deletion of β 6, and consequently α β 6, protected against bleomycin induced pulmonary fibrosis suggesting its role in TGF- β 1 activation (Munger et al. 1999). However, bleomycin does not fully recapitulate human IPF, which may have myofibroblasts that express more than just α β 6 integrin. The deletion of α β 3, α β 5 or α β 6 subunits failed to protect against liver fibrosis highlighting the idea that there may be compensatory β integrins involved in TGF- β 1 activation. On the other hand, blockage of the α portion of these integrins prevented the development of fibrosis (Henderson et al. 2013). Overall, the ECM stiffness effect on TGF- β 1 activation through integrin binding leading to eventual fibroblast to myofibroblast differentiation highlights a complex network that helps promote myofibroblast differentiation.

1.4 Cell culture models to elucidate lung ECM effects on fibroblast and myofibroblast phenotype

1.4.1 2D plastic cell culture system

Ramos et al. (2001) showed IPF fibroblasts have an increased expression of α -SMA compared to normal fibroblasts; protein expression of α 1 collagen and TGF- β 1 was elevated in IPF fibroblasts compared to normal fibroblasts. Furthermore, they demonstrated that the growth rate for IPF fibroblasts was lower than normal fibroblasts.

Overall, comparison of normal and IPF fibroblasts grown on 2D plastic revealed differences in phenotype, even though this study model lacks the spatial cues, ECM components, and growth factors that would be present in the 3D native lung.

1.4.2 2D silicone soft and stiff culture system

Balestrini et al. (2012) explanted and passaged rat lung fibroblasts on varying silicone stiff cell culture plates. They found an increase in myofibroblast differentiation when normal lung explants were grown on stiff silicone plates compared to soft plates. This differentiation of fibroblasts into myofibroblasts was analyzed based on levels of α -SMA immunostaining. Furthermore, their results indicated that fibroblasts and myofibroblasts retained their mechanical memory; identifying that when fibroblasts were grown on stiff silicone and then reseeded onto softer silicone plates they retained their myofibroblast phenotype. When normal fibroblasts were transferred from soft to stiff silicone plates, they retained their normal phenotype. Liu et al. (2010) utilized stiff and soft culture plates as well and they showed that stiffer cell culture plates induced α -SMA positive myofibroblast population compared to a softer cell culture plates. These experiments indicate that myofibroblasts obtain an irreversible α -SMA phenotype. However, the major limitation to this culturing method was that they did not recapitulate the 3D spatial cues and binding domains from the microenvironment found in native lung ECM. Another limitation would be that evaluation of phenotype changes following 4 days or 1 passage might not be sufficient time to fully evaluate whether changes in substrate stiffness could eventually induce phenotype changes. An important result that should be taken away from these studies is that regardless of the source of the lung,

explanting a normal lung on stiff plastic induces α -SMA majority myofibroblast population.

1.4.3 3D collagen gel cell culture system

A review done by Hinz et al. (2007) highlights the effects that culturing fibroblasts in soft and stiff 3D collagen gel has on fibroblast phenotype. When fibroblasts were seeded into a soft collagen gel, the fibroblast did not differentiate into myofibroblasts. On the other hand, when fibroblasts were seeded into a stiff 3D collagen gel there was an increase in fibroblast to myofibroblast differentiation. One limitation of this experiment would be that a gel consisting of only collagen might signal a profibrotic environment contributing to the differentiation of fibroblast to myofibroblast.

1.4.4 Native lung ECM as a 3D cell culture system

The development of methods to isolate native lung ECM and culture fibroblasts/myofibroblasts within this ECM was needed in order to fully study the role lung ECM has on fibroblast/myofibroblast phenotype. Isolation of lung ECM was required and one of the ways to achieve this was through decellularization of lung, which leaves behind only the lung ECM. Decellularization has been achieved with three main detergents SDS, SDC, and CHAPS (3-[(3-cholamidopropyl)dimethylammonio]-1-propanesulfonate). Decellularized lung ECM provides a natural material that contains natural binding sites and spatial cues found in a native lung. This lung ECM can be reseeded with fibroblasts from both normal and IPF lung-derived biopsies. Booth et al. (2012) used this fibroblast culturing method and found that normal fibroblasts modulated their phenotype to the lung matrix that they were reseeded on, normal or fibrotic. This

result suggests that fibroblast/myofibroblast phenotype was not permanent, which was contradictory to the result obtained when fibroblasts were reseeded onto varying silicone stiffness.

1.5 Purpose of study and hypothesis

The purpose of the thesis was to examine lung ECM effects on myofibroblast phenotype. As outlined previously, there was contradictory evidence on whether or not lung ECM can induce a permanent myofibroblast phenotype, and whether or not this phenotype could be reversed. In order to examine this relationship, development of methods to isolate lung ECM and culture of myofibroblasts within this matrix had to occur in order to answer whether lung ECM alone can modulate myofibroblast phenotype.

Isolation of lung ECM through decellularization had not been carried out in our labs prior to this thesis driving the development of a method that consistently decellularized lung. Furthermore, throughout this thesis, it became apparent that the effectiveness of lung ECM isolation through decellularization and methods of culturing on decellularized lung ECM had to be explored so that the model being used reflected, as close as possible, *in vivo* conditions.

Hypothesis:

We hypothesize that fibroblast/myofibroblast will adopt the phenotype of the lung ECM that they are cultured on. For example, IPF-derived myofibroblasts will adopt a quiescent-like fibroblast phenotype when cultured on normal lung ECM.

Chapter 2: Materials and Methods

2.1 Lung Explant

Human fibroblast cell lines were derived using the fibroblast explant method. Control lung biopsies were obtained from morphologically normal lung of carcinoma patients undergoing resection. Similarly, IPF lung biopsies were obtained from IPF patients undergoing resection. Lung biopsies were then explanted from respective patients; the lung tissue was minced into fine strips where they were plated on a sterile cell culture dish. The lung tissue was held down on the culture dish using a sterile coverslip held in place with sterile Vaseline. Next, RPMI (Lonza, 12-702F) supplemented with 10% FBS (GIBCO), 100U penicillin/streptomycin (GIBCO), and 0.2% Amphotericin B (Lonza) was carefully added to the dish by running the medium down the edge until the lung fragments were covered. Media was changed every week until the migration of fibroblasts out of lung tissue fragments was complete.

2.2 Soft plate cell culture

Soft plates were obtained from Matrigen (SS6-COL-1). Hydrogels bound to glass coverslips with a stiffness of 1 kPa coated with collagen-I was inserted into 6 wells cell culture plates.

2.3 Animal Experiments

Female Sprague Dawley (SD) rats were obtained from Charles River (225g-250g). Rats were harvested at 110-120 days old.

2.4 Lung slice elastance

A 3D horizontal tissue bath was constructed with dimensions 3x1x1cm. A force transducer and a servo-control arm were used in tandem with a digital controller interface (Models 400A, 322C, 604C, Aurora Scientific Inc.). Trimmed tissue strips were pasted to metal clips via ethyl 2-cyanoacrylate based adhesive (Electron Microscopy Sciences, Inc.) and attached to a hook on the force transducer and servo-arm in the tissue bath. Static tissue elastance was measured by reading the force one second before and one second after a length increase of 0.01 times the resting tissue length. Elastance was calculated with the formula: $(\text{force (2)} - \text{force (1)}) / (\text{length (2)} - \text{length (1)})$ and expressed in mN/cm. The initial tissue tension for the static elastance test was set to 5mN.

2.5 Western Blot analysis

30 µg of protein was loaded into a 10% or 14% sodium dodecyl sulfate-polyacrylamide gel electrophoresis (SDS-PAGE). Proteins were blotted onto a polyvinylidene difluoride (PVDF) membrane, blocked 1 hour in 5% dry milk/TBS-0.1% Tween 20, and incubated with primary antibody at 4°C overnight. Secondary HRP-conjugated antibodies were applied for 1 hour at room temperature. Blots were developed with ECL reagent and imaged using ChemiDoc MP imager and Image Lab software (Bio-Rad). Antibody concentrations were: 1:2000 for rabbit anti-glyceraldehyde 3-phosphate dehydrogenase (GAPDH) (Cell Signaling Technology #5174), 1:2000 rabbit anti-alpha smooth muscle actin (Abcam ab5694), 1:1000 rabbit anti-caspase 3 (Cell Signaling Technology #9662), 1:1000 rabbit anti-α tubulin (Cell Signaling Technology #2144), and 1:1000 anti-rabbit IgG (Cell Signaling Technology #7074).

2.6 Histology

After a given incubation period, reseeded lung slices were fixed in 10% buffered formalin for histological assessment. Lung slices were subsequently paraffin embedded and 4 µm sections were made. Sections were deparaffinized using successive bathing of Xylene, ethanol 100%, ethanol 95% and ethanol 70% and stained using hematoxylin and eosin (H&E), elastic tissue fibers-Verhoeff's-Van Gieson (EVG), picro sirius red (PSR), Miller's elastic fiber, and Masson's trichrome.

2.7 Immunohistochemistry, Immunocytochemistry and immunofluorescence

Lungs were fixed in 10% formalin and cells were fixed in 4% paraformaldehyde. Lungs were then paraffin embedded and 4 µm sections were cut. Lung sections were deparaffinized using successive bathing Xylene, ethanol 100%, ethanol 95% and ethanol 70%. Endogenous peroxidases were inhibited by 1% H₂O₂ in lung sections and cells. Lung section antigens were exposed through steaming the lung slice in citrate buffer (10 mM citric acid, 10 mM sodium citrate, pH 6.0). Next, antigens were blocked with 0.3% BSA diluted in PBS for 1 hr. Lung sections and cells were then incubated with primary antibody 1:100 Rabbit anti-alpha smooth muscle actin (Abcam ab5694) overnight at 4°C. Finally, 1:1000 anti-rabbit IgG (Cell Signaling Technology #7074) secondary antibody was added for 1 hr at room temperature and peroxidase was revealed using Vector NovaRED (Vector Laboratories). Sections and cells were counterstained using Mayer's hematoxylin.

For immunofluorescence, the same protocol was used but lung sections and cells (cultured on coverslips) were treated with 0.1% Sudan black for 30 minutes to reduce

auto-fluorescence. 1:100 anti-vimentin (Cell Signaling Technology #5741) and anti-alpha smooth muscle actin antibody (Abcam ab7817) were incubated at 4°C overnight. Next, 1:1000 anti-rabbit IgG (Abcam ab150080) and anti-mouse IgG (Abcam ab150113) secondary antibodies were added for 1 hr at room temperature and then Prolong Gold antifade reagent with DAPI (P36931 life technologies) was used to stain nuclei and mount the coverslips.

2.8 Statistics

Statistics were done using Graphpad. The data were expressed as mean \pm SEM (all error bars represent \pm SEM). Where appropriate an unpaired, 2-tailed Student's t test was performed to evaluate experimental groups.

Chapter 3: Development of Methods to Elucidate Lung ECM Effects on Fibroblast/Myofibroblast Phenotype

3.1 Aims

- 1) Develop a decellularization protocol that consistently decellularized rat lungs
- 2) Develop a method to effectively reseed decellularized rat lungs
- 3) Compare lung decellularizing detergents

3.2 Decellularization and Reseeding of Lung Slices

3.2.1 Background

The process of decellularizing a rodent lung had not been carried out in our labs and one of the objectives of this project was to provide an initial foundation of knowledge for decellularizing rodent lungs. Nonetheless, previous work done in our labs involved inflating rodent lungs with agarose and cutting ~300 µm lung slices on a vibratome in order to image them. Additionally, a decellularization protocol was given to us through a collaborator, which involved decellularizing 50 µm lung slices using a combination of reagents: SDS, EDTA and NaCl. Since the goal of this project was to examine lung ECM effects on fibroblast phenotype, it was decided that 50 µm thickness was not appropriate to mimic 3D ECM leading to the use of a thicker the 300 µm lung slice.

3.2.2 Decellularization Protocol

Sprague Dawley rats were euthanized with CO₂. The skin overlaying the abdomen and thorax was reflected to expose the abdomen and thorax. The liver and intestines of the animal were reflected out of the way to expose the diaphragm and then the descending aorta was cut to drain blood out of the vasculature. Next, a careful incision was made to

the bottom of the left rib cage in order to pierce the diaphragm and deflate the lungs. Then, the sternum was cut all the way to the neck region. The salivary glands and thyroid were removed to expose the trachea. After that, an incision was made in the trachea, near the larynx, so that a blunt 16-gauge needle could be inserted. Additionally, a blunt 16-gauge needle was inserted into the right ventricle in order to perfuse lung vasculature through the pulmonary artery. Heart and lungs were excised en bloc and the lungs were inflated with 2% low melting agarose and were cut using EMS-4000 vibratome. It was determined, through experimentation, that 300- μm thick lung sections was an optimal thickness. Next, lung slices were placed in a 35mm cell culture dish and decellularized using a solution containing: 1) 0.1% SDS, 25mM EDTA, and 1M NaCl. Lung slices were incubated in the decellularization solution for 72 hrs on a rocker at 4°C. At the 23 and 47 hr time points, the lung slices were washed with ddH₂O for 1 hr at 4°C, and decellularization solution was reapplied. After the incubation period, each lung slice was washed with 1X PBS solution, and then incubated in a 30 $\mu\text{g}/\text{mL}$ DNase I solution for 10 mins. Next, the lung slices were washed with 1XPBS followed by incubation in 0.1% Triton-X 100 for 15 min. Finally, lung slices were washed three times in 1XPBS.

3.2.3 Reseeding Protocol

Drop-wise reseeded was performed through a method derived from Booth et al.'s work (2012). First, the 300 μm decellularized lung slices were washed for 5 mins in 0.18% peracetic acid and 4.8% ethanol in ddH₂O, and then they were washed with RPMI for ~1 hr in a 37°C, 5% CO₂, 95% O₂ incubator. RPMI was aspirated off and lung slices

were left in a biosafety cabinet to dry. Once dry enough, the lung slices were ready for reseeded of ~50,000 cells per decellularized lung slice.

3.2.4 Results

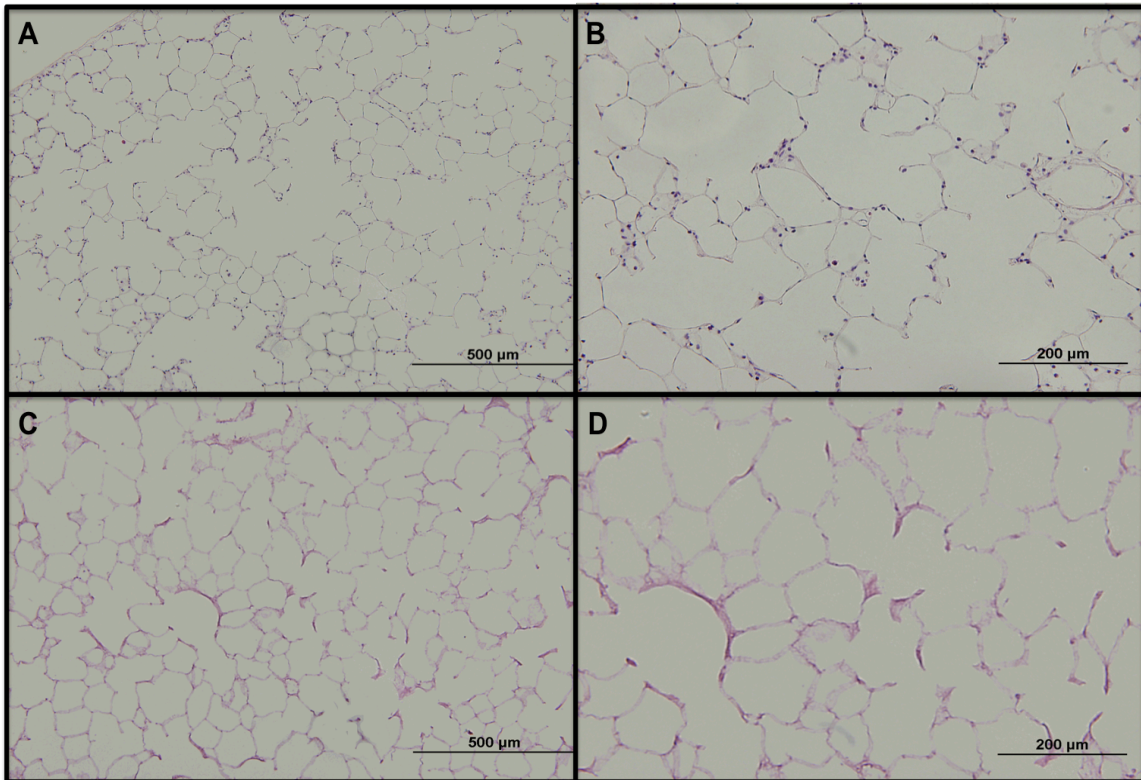


Figure 3-H&E staining of decellularized lung slices

A and **B** represent normal lung slices at 100X and 200X. The presence of cells indicated by the dark purple stain. **C** and **D** represent decellularized lung slices that were noticeably free of cells. Lung slices were fixed in 10% formalin, paraffin embedded, and cut at 4 μ m thick. Decellularization of rat lung slices with 0.1% SDS, 1M NaCl, and 25 mM EDTA was clearly effective, which was evident in figure 3. When comparing normal lung to decellularized lung slices, there appeared to be distortion or ruffling of the ECM (figure 3 B and D).

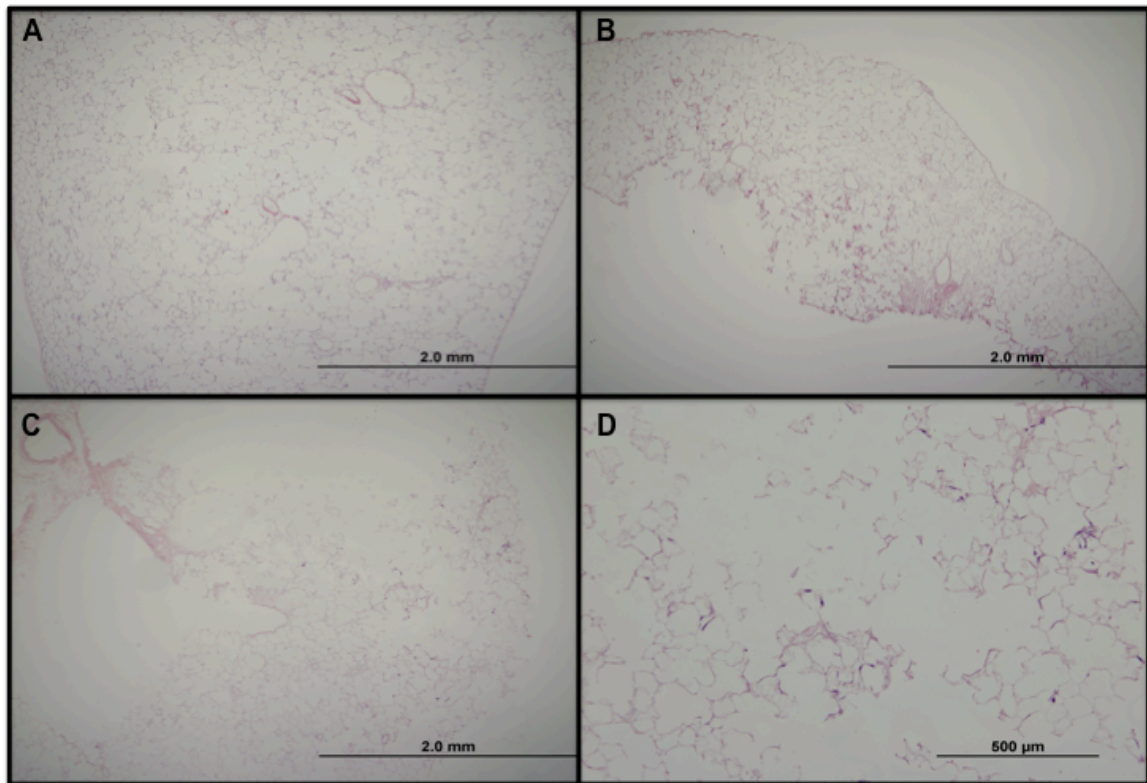


Figure 4-H&E staining of reseeded decellularized lung slices

A represents H&E staining of a normal lung at 4X magnification. B and C represents H&E staining of reseeded decellularized lung slices at 40X, and D magnifies the reseeded area shown in C. Notice the presence of cells indicated by the dark purple stain. Morphology of reseeded lung slices was poor in comparison to a normal lung. Lung slices were fixed in 10% formalin, paraffin embedded, and cut at 4 μm thick.

Paraffin sectioning of reseeded lung slices proved to be difficult and lead to sections that had poor morphology. Furthermore, reseeding fibroblasts using the drop-wise method resulted in lung slices that had sporadic reseeding. The images in figure 4 were the select few reseeded lung slices that could be paraffin sectioned and were actually reseeded, but most lung slices were either unable to be paraffin sectioned or had no evident fibroblast reseeding.

3.2.5 Discussion

Decellularization of rat lung slices was eventually achieved through many modifications. The extension of decellularizing time from 24 hr to 72 hr and the addition of ddH₂O at 23 hr and 47 hr time points were essential to achieve full decellularization. One of the major drawbacks to this method was that cutting an intact native lung into a hundred individual lung slices for decellularizing was inefficient and cumbersome. This was quite evident when initial reseeding experiments were carried out.

Additionally, Booth et al.'s drop-wise reseeding technique resulted in lung slices that were inconsistently reseeded (figure 4D). More importantly and critical for evaluating lung ECM on myofibroblast phenotype, paraffin sectioning of reseeded lung slices proved to be an onerous challenge due to the thin lung slice beveling within the paraffin wax. Unreliable paraffin sectioning was a major issue that had to be addressed and led to the pursuit of a more reliable decellularization method.

3.3 Whole Rat Lung Decellularization and Reseeding

3.3.1 Background

The previous decellularization method led to the pursuit of a less burdensome decellularization method that would decellularize one intact whole lung instead of creating tens of lung slices to decellularize. Whole lung decellularization will allow for multiple avenues to study lung ECM effects on fibroblasts/myofibroblasts phenotype. For example, whole lung decellularization would allow the lung to be reseeded and then sliced into lung slices for static culture or could be reseeded and hooked up to a lung bioreactor for biomimetic culture. There have been numerous whole lung decellularization protocols to date utilizing mouse, rat, porcine, macaque and human lungs. These decellularizing protocols have primarily used one of SDS, SDC, and CHAPS as their main decellularizing agents. Ott et al. (2010) successfully decellularized a rat lung via perfusion of 0.1% SDS through the pulmonary artery. Petersen et al. (2010) perfused CHAPS through the pulmonary vasculature to decellularize a whole rat lung. However, it was quite evident that SDC was the most widely used whole lung decellularizing agent; SDC had been used to decellularize whole mouse, rat, monkey, and human lungs (Price et al. 2010; Bonvillain et al. 2012, Booth et al. 2012, Daly et al. 2012, Jensen et al. 2012). Ultimately, SDC was chosen as the detergent to decellularize whole rat lung.

3.3.2 Decellularization Protocol

Isolation of rat lungs was identical to the procedure described for decellularizing rat lung slices. Following isolation, the lungs were perfused by injecting 10 cc of ddH₂O

solution through the pulmonary artery. Next, the lungs were inflated with 10 cc of ddH₂O solution through the trachea, and then the ddH₂O solution was contained in the lungs by tightening a suture around the trachea. The lung was kept at 4°C for 1 hr in ddH₂O solution. The rest of the rinses and washes were done with a 20 mL syringe and a 16-gauge needle in a sterile 100mm dish as follows:

1. Remove lungs from solution. Inject five rinses of 10 cc of ddH₂O through the trachea and five 10 cc of ddH₂O through the pulmonary artery. Remove syringe after each injection to allow solution to come out based on lung's natural recoil.
2. Inject 10 cc of 0.1% Triton-X 100 into the lungs through the trachea and pulmonary artery. Incubate for 24 hrs at 4°C.
3. Repeat step 1.
4. Inject 10 cc of 2% sodium deoxycholate into the lungs through the trachea and pulmonary artery. Incubate for 24 hrs at room temperature.
5. Repeat step 1.
6. Inject 10 cc of 1M NaCl into the lungs through the trachea and pulmonary artery. Incubate for 1 hr at room temperature.
7. Repeat step 1.
8. Inject 10 cc of 30 µg/mL DNase I from bovine pancreas through the trachea and pulmonary artery. Incubate for 1 hr at room temperature.
9. Repeat step 1.
10. Repeat rinses from step 1 with 1X phosphate buffered saline

*All solutions contained 100U Penicillin/Streptomycin.

3.3.3 Reseeding Protocol

Whole lung method of reseeded with cells mixed with agarose was adopted from previous works (Bonvillain et al. 2012, Daly et al. 2012, Scarritt et al. 2014). Prior to reseeded, the decellularized lungs were washed with RPMI. Fibroblasts were detached from tissue culture plates using 0.5% Trypsin-EDTA and cell concentration was adjusted to 2 million cells/mL in RPMI prior to reseeded. Next, sterile 1% agarose made in media was mixed with the cell suspension creating a solution containing 1 million cells/mL. This solution was then injected into the lungs through the trachea. The lungs were put in a 4°C fridge for 15 mins to allow for solidification of the agarose. Finally, the inflated lungs were cut into ~1-2 mm thick lung slices, which were cultured in a 12 well plate for desired incubation period. Media was changed every other day.

3.3.4 Results

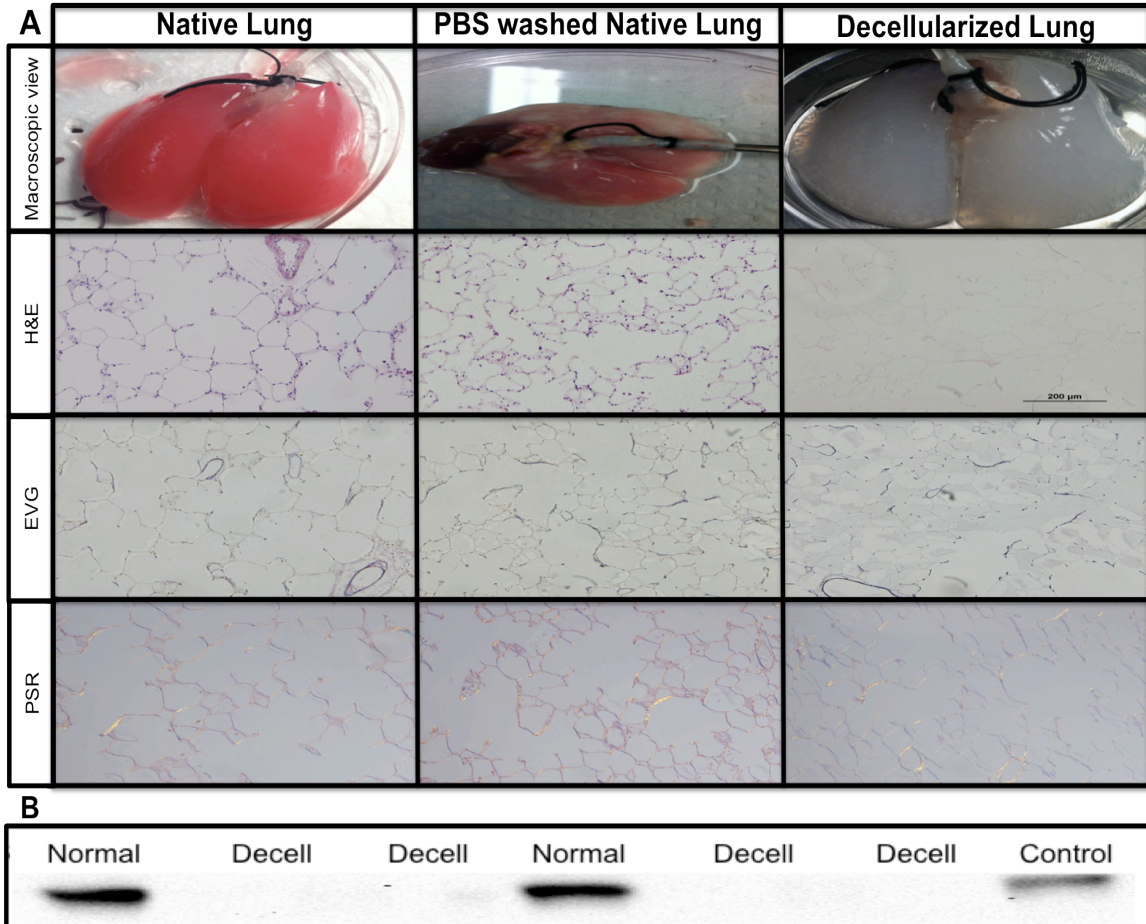


Figure 5-Macroscopic, histologic, and western blot analyses of normal freshly fixed, PBS washed, and decellularized whole rat lungs

A Comparison of H&E, EVG, and PSR staining between freshly fixed normal lung, PBS washed lung, and decellularized lung were made. Examining the H&E row, both freshly fixed normal lung and PBS washed lung have cells that are present depicted as dark purple stain whereas decellularized lung slice was free of cells. Examination of EVG and PSR staining, that ECM components were retained following decellularization shown by retention of black elastic fibers stained black in EVG and polarized yellow collagen fibers

in PSR stain. Lung slices were fixed in 10% formalin, paraffin embedded, cut at 4 μ m thick, and viewed at 200X objective. **B** Western blot of intracellular protein α -tubulin was performed to further demonstrate full decellularization.

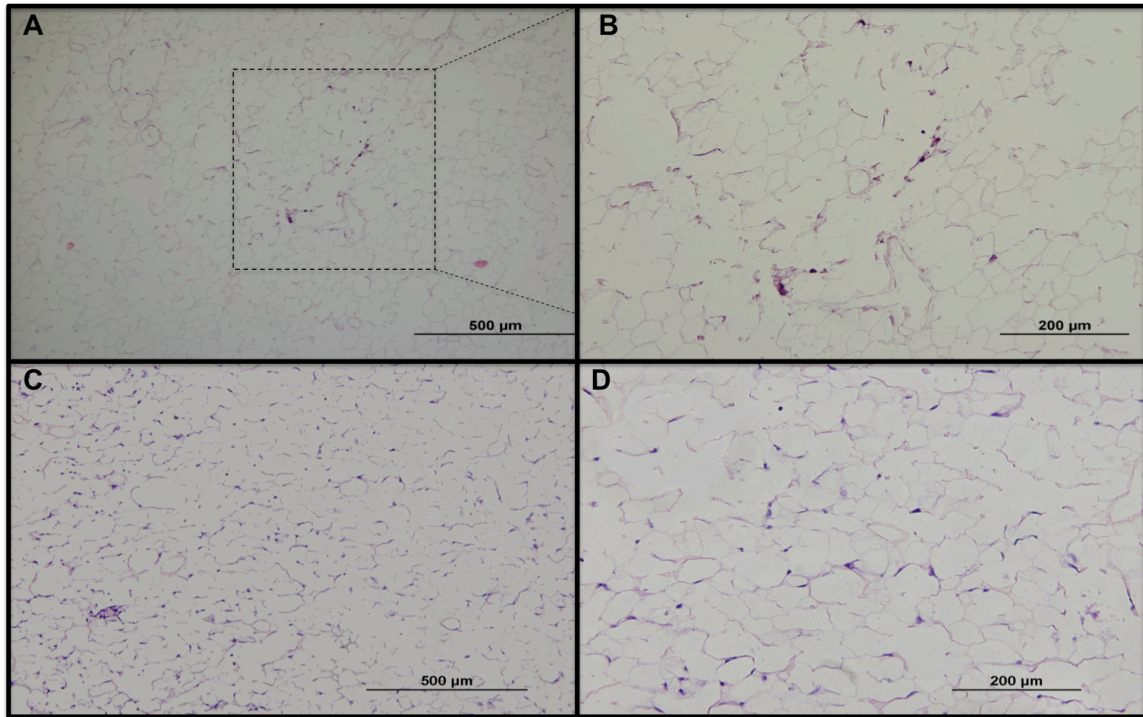


Figure 6-Comparison of drop-wise and whole lung reseeding techniques

A and **B** represents drop-wise reseeding technique conducted on 1000 μ m thick lung slices cut from a decellularized whole lung. The drop-wise reseeding technique shown here was the only position within the lung slice that had fibroblasts present. **C** and **D** represents whole lung reseeding technique of mixing fibroblasts with 1% agarose, notice the consistent presence of fibroblasts compared to the drop-wise reseeding technique. Lung slices were fixed in 10% formalin, paraffin embedded, and cut at 4 μ m thick.

Reseeding of decellularized of 1000 μm thick lung slices cut from a decellularized whole lung resulted in inconsistent reseeded (figure 6 B). The H&E images illustrating the drop-wise reseeded technique were the best images, however, majority of lung slices were absent of fibroblasts. Conversely, when implementing the whole lung reseeded technique (Bonvillain et al. 2012, Daly et al. 2012, Scarritt et al. 2014), it was evident that inflating the decellularized lung using the whole lung reseeded of fibroblasts mixed with agarose was a superior reseeded technique.

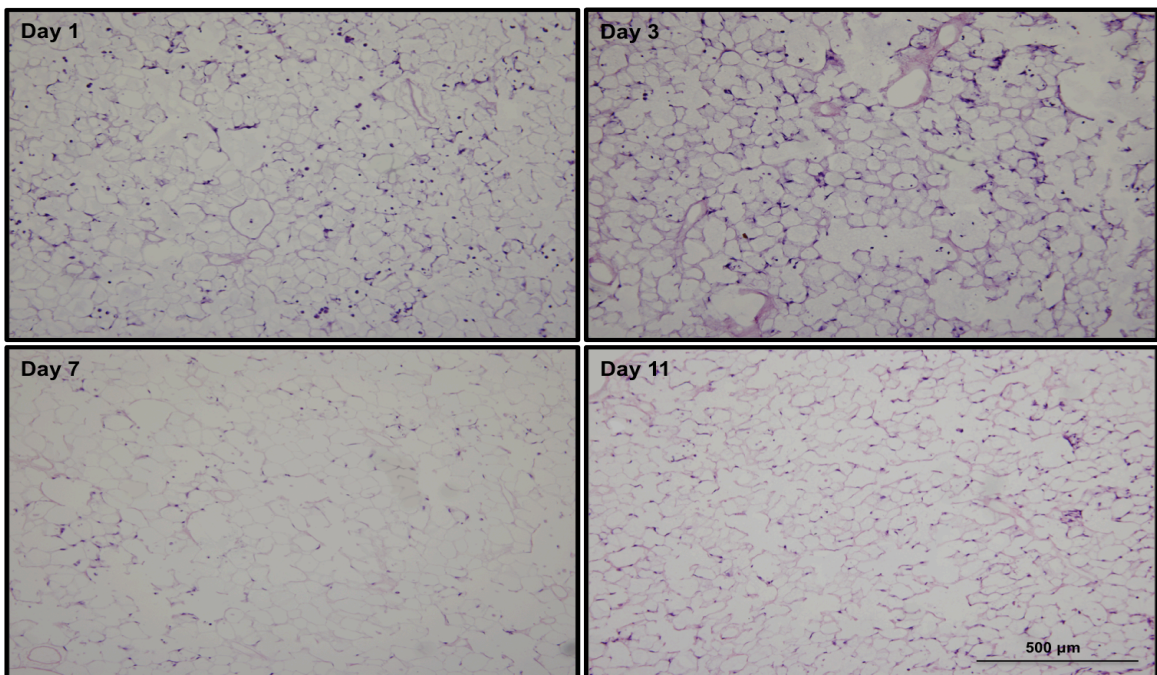


Figure 7-Timeline of fibroblast migration out of agarose onto decellularized whole rat lung ECM

Day 1-11 demonstrates the migration of fibroblasts out of agarose and onto lung ECM through H&E staining. At day 1, most of the fibroblasts are spherical and still embedded in the agarose, but by day 3 the majority of the fibroblasts have attached to the lung ECM. Days 7 and 11 confirm that all fibroblasts have migrated out of the ECM and were viable

for at least 11 days in culture. Lung slices were fixed in 10% formalin, paraffin embedded, and cut at 4 μ m thick.

3.3.5 Discussion

The first two objectives of this thesis: i) development of a decellularization protocol that consistently decellularized rat lungs and ii) effectively and efficiently reseed decellularized rat lungs were successfully achieved through the whole lung decellularization and reseeded technique. The inconsistency of the drop-wise reseeded technique was mystifying; attempts to improve this technique were explored, like increasing initial fibroblast incubation time, but all attempts failed to provide better results. Furthermore, the whole lung reseeded technique provided consistent results when multiple primary fibroblast cell lines were used. It was concluded, based on these results, that whole lung decellularization and reseeded technique would be the optimal strategy to elucidate lung ECM's effects on fibroblast phenotype.

The whole lung decellularization protocol utilized SDC as the main detergent lasting 50 hrs, in contrast, decellularizing lung slices with SDS as the main detergent lasted 72 hrs. In regards to aim 3, comparison of decellularizing agents, there were no comparisons attempted to evaluate the effectiveness of the respective decellularizing detergents because the route of administration and length of decellularizing times were dissimilar. To impartially compare decellularizing agents there had to be development of an apparatus that would deliver decellularizing agents in the same manner and at a constant pressure.

3.4 Rapid whole lung decellularization

3.4.1 Background

Wallis et al. (2012) conducted a study examining the effectiveness of CHAPS, SDS, and SDC at decellularizing mice lungs with an aim at determining which decellularizing agent was best. They concluded that there was not a superior decellularizing agent, even though ECM differences arose following decellularization, because the respective decellularized ECM could be effectively reseeded. One limitation to this conclusion was that only C10 epithelial cells were reseeded, but different cell types may potentially respond differently to the detected changes in ECM composition. Also, it was worth noting that they manipulated decellularizing protocols to reflect the protocol used by Price et al. (2010), which may have improved or hindered the decellularizing agent's effectiveness.

Gilpin et al.'s (2014) study also compared CHAPS, SDS, and SDC effectiveness at decellularizing rat lungs. They administered detergents at a constant pressure of 30 cmH₂O through the pulmonary artery. The rapid decellularization method was modeled after Gilpin et al.'s (2014) and Calle et al.'s (2011) work since they both used methods that controlled the pressure at which detergents were administered. Controlling the pressure at which decellularization solutions were administered was important so that perfusion pressure did not confound the ability to compare each detergent's ability to retain lung ECM. In contrast to Gilpin et al.'s work that used 30 cmH₂O to perfuse the lungs, the rapid decellularization method presented in this thesis used a perfusion pressure of 20 cmH₂O (Calle et al. 2011). Additionally, CHAPS was not evaluated in this thesis

due to the price being 35 times the price of SDS and 24 times the price of SDC making it a detergent that was impractical when decellularizing many lungs.

Determining which detergent would be most effective, it was hypothesized that SDC would retain more lung ECM in comparison to SDS. This hypothesis was based on the molecular properties of SDC; SDC is a fat emulsifier by trade and is used to isolate membrane bound proteins. On the other hand, SDS is an anionic detergent used to denature proteins. According to ThermoScientific's website, the critical micelle concentration of SDS is 0.1728 to 0.2304%, w/v, which was close to the 0.1% SDS concentration used in previous lung decellularization protocols. On the other hand, the critical micelle concentration of SDC is 0.083 to 0.249%, w/v, which is ~10 times less than the actual concentration of SDC used in published papers (2%) (Price et al 2010, Bonvillain et al. 2012, Daly et al. 2012, Gilpin et al. 2014). From this information it was further hypothesized that a reduction in SDC would be equally effective at decellularizing rat lungs compared to the traditional 2% SDC. It is critical to isolate intact native lung ECM that resembles *in vivo* ECM in order to properly study and infer lung ECM effects on fibroblast/myofibroblast phenotype.

In theory, the rapid decellularization method could be automated allowing the user to set up multiple lungs to be decellularized at once and then return upon completion of decellularization. This protocol would allow the researcher to decellularize and reseed within the same day, which would be an improvement on previous work where a decellularized lung would be put in a fridge for weeks to a month waiting to be reseeded.

3.4.2 Decellularization Protocol

Lungs were processed as previously described; the lungs were flushed with 1XPBS to remove excess blood and then inflated with ddH₂O until further processing.

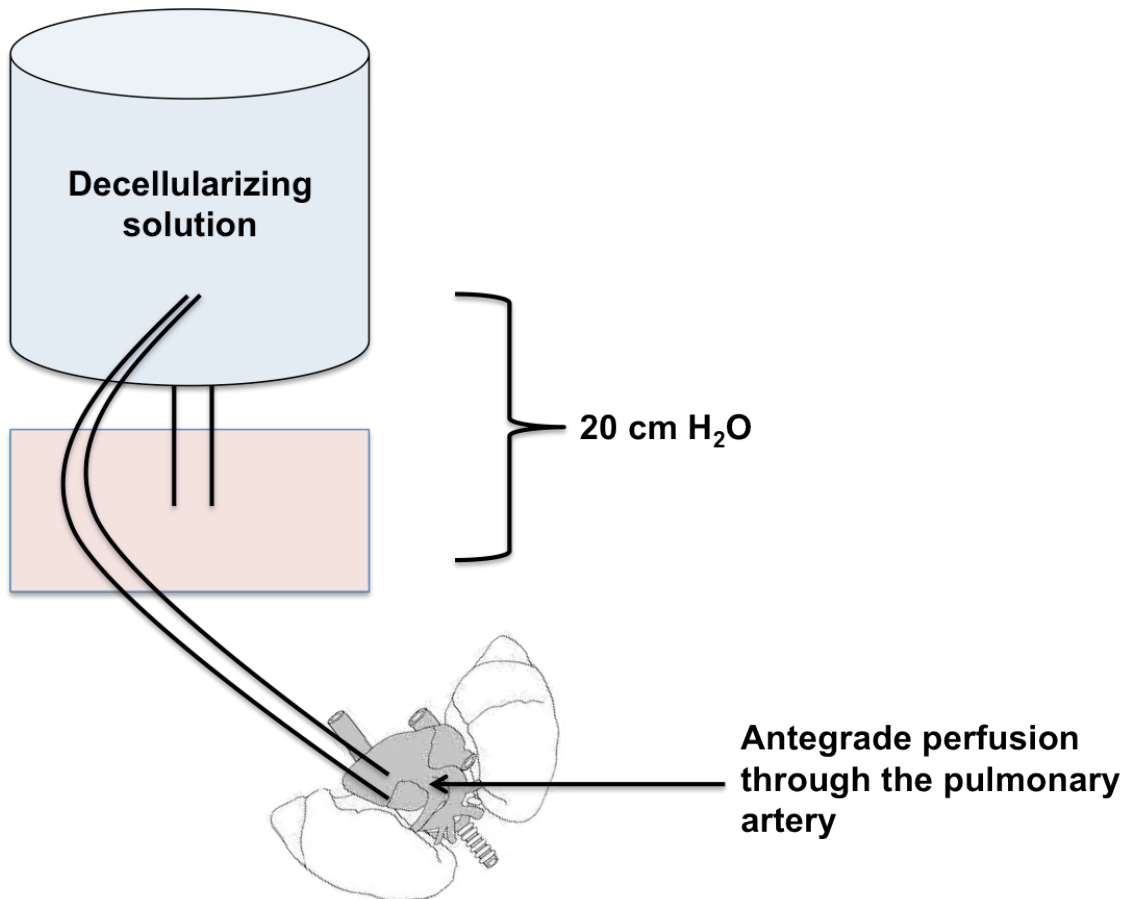


Figure 8-Schematic of rapid whole lung decellularization set-up

The pulmonary artery was cannulated with a 16-gauge needle and attached to a male luer lock adapter connecting to a reservoir of decellularizing detergents. It was crucial to have no air bubbles within tubing from reservoir to pulmonary artery in order to have continuous flow of solutions. The following were the decellularizing steps for each respective protocol.

SDC Decellularizing steps:

1. 1XPBS for 10 mins
2. 0.1% Triton X-100 for 30 mins
3. Main detergent was 2% or 0.5% SDC until visually decellularized
4. 1M NaCl for 30 mins
5. Perfusion of ddH₂O and 1XPBS through the pulmonary artery and trachea five times

SDS Decellularizing steps:

1. 1XPBS for 10 mins
2. 0.1% SDS until visually decellularized
3. ddH₂O for 15 mins
4. 1% Triton X-100 for 10 mins
5. Perfusion of ddH₂O and 1XPBS through the pulmonary artery and trachea five times

3.4.3 Preliminary Results

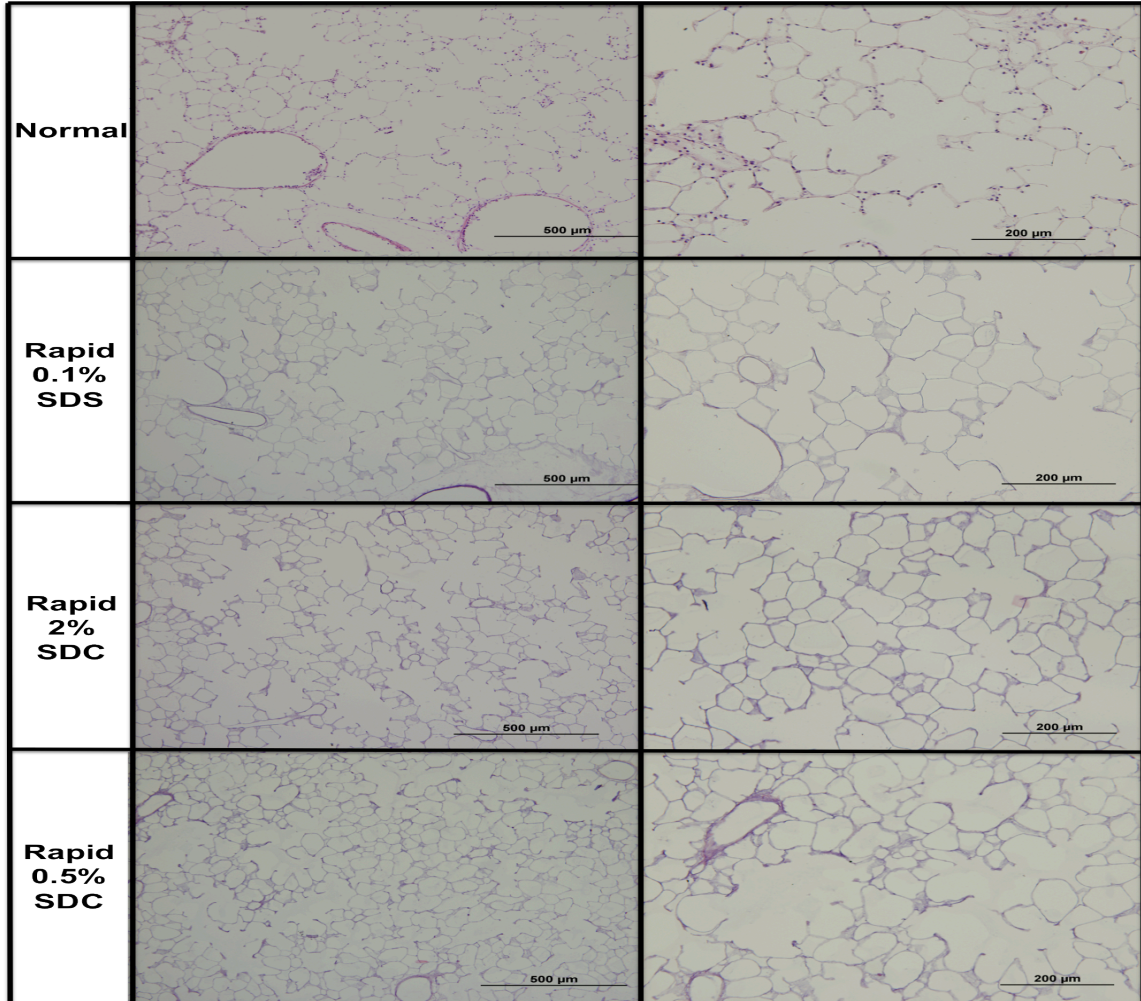


Figure 9-Histological comparison of various decellularizing agents utilizing rapid decellularization technique

H&E results for rapid decellularization demonstrate that this technique was successful in decellularizing whole rat lungs. Images were taken 10X and 20X magnification. All detergents effectively decellularized whole rat lungs, and interestingly, the 0.5% SDC appeared to be as equally effective at decellularizing rat lungs. On average it took 4-5 hrs to complete the rapid decellularization.

3.4.4 Comparison of ECM following rapid decellularization

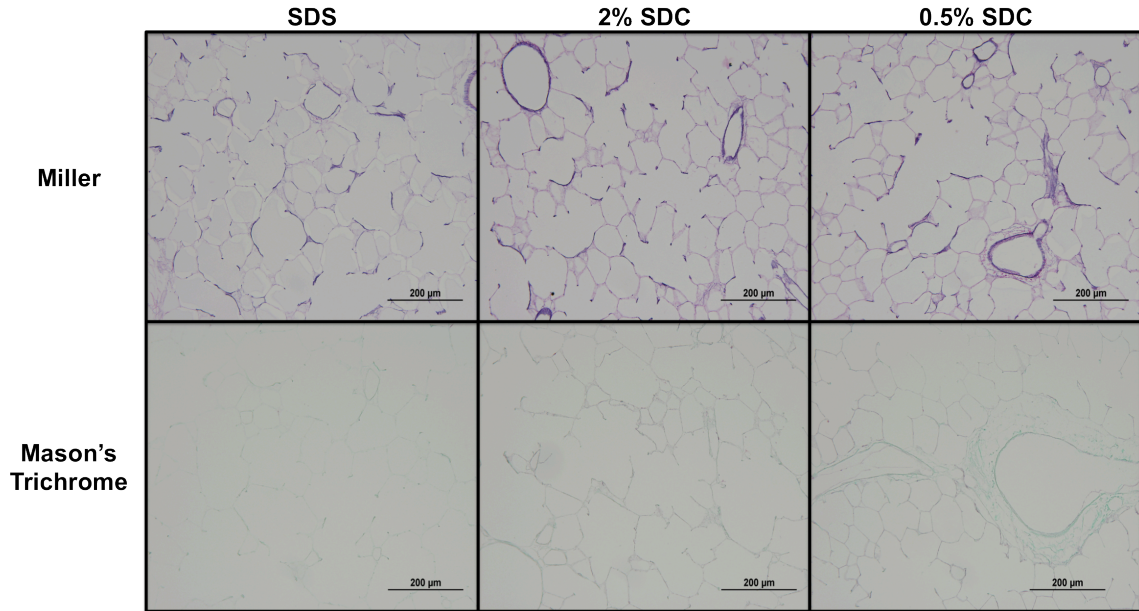


Figure 10-Histological comparison of decellularizing agent's effects on retaining lung ECM following rapid decellularization

All images were taken at 20X magnification. The top row represents Miller's elastic staining protocol, which stains elastic fibers black, collagen red, nuclei brownish green, and erythrocytes yellow. Only the black elastic fibers and the red collagen fibers were present following staining. It would appear that both concentrations of SDC retain more elastic and black fibers compared to the SDS detergent. The second row represents Masson's trichrome staining where collagen was stained blue and nuclei stained black. It was quite noticeable that the SDC retained more collagen following decellularization than SDS, and the 0.5% concentration of SDC was best at retaining collagen.

3.4.4 Discussion

The set-up of rapid lung decellularization achieved full decellularization using different detergents supporting its usefulness as a tool for decellularization. This set-up allowed for control over route of detergent administration and input pressure at which the detergent was delivered. Controlling for these two factors was crucial in order to impartially compare the effectiveness of different detergents at decellularizing and retaining native ECM.

H&E staining demonstrated that all three decellularizing protocols achieved full lung decellularization. Histological evaluation of collagen and elastic fibers in decellularized ECM revealed that SDC was far superior at retaining lung ECM following decellularization compared to SDS (figure 10). This result supports the hypothesis that SDC would be better at retaining the ECM proteins due its chemical properties as a fat emulsifier compared to a protein-denaturing agent SDS. The second hypothesis was that a reduction of SDC concentration from 2% would be equally effective at decellularizing whole rat lung since 2% concentration was 10 times higher than the critical micelle concentration of SDC. H&E staining showed that 0.5% SDC concentration could decellularize whole rat lung, and based on Miller's and Trichrome staining it would appear that SDC at this concentration was most effective at retaining lung ECM as well.

Future work will need to further quantify differences in lung ECM post decellularization. However, beyond comparing the effectiveness of decellularizing detergents, the rapid decellularization set-up would be an optimal method to use when reseeding decellularized whole lungs. Rapid decellularization would allow the user to

match cell cultures with decellularization. This would be an improvement from the manual whole lung decellularization that lasted 50 hrs, which did not allow for seamless decellularization and reseeding on the same day.

The detergent that can retain lung ECM resembling native composition and conformation the best following decellularization will potentially improve the ability to successfully regenerate a lung. Studying lung ECM effects on fibroblast or myofibroblast phenotype requires the isolation of native lung ECM that is not damaged since this could produce undesired results. Furthermore, regeneration of a lung through decellularization of a donor lung and reseeding with host stem cells will require optimal lung ECM-cell engraftment as well. The decellularizing detergent chosen may impact more than simply removing cellular material; the detergent has to maintain native lung ECM components and conformation as close as possible. Reseeding of a decellularized lung requires an ECM scaffold that will provide appropriate cell binding domains and spatial cues permitting correct cell differentiation and proliferation. All of these processes are required in order to fully elucidate lung ECM effects on cell phenotype.

3.5 Lung Bioreactor Design and Culture

3.5.1 Background

The purpose of building a lung bioreactor was to provide a biomimetic culturing device that simulated physiological ventilation and vascular perfusion of the lungs. The previous reseeding of decellularized whole lungs would be considered a static culturing method since there was neither physiological respiration nor vascular perfusion. Concerns of whether or not agarose within the static lungs slices was influencing the ability to fully elucidate lung ECM effects on fibroblast/myofibroblast phenotype drove the development of a biomimetic culture method. The hypothesis is that the lung ECM's effect on the fibroblast phenotype resulting from static lung culture would be similar when cultured in a biomimetic device or lung bioreactor.

The development of a lung bioreactor required three basic apparatuses: a ventilation unit, a vascular perfusion pump, and a unit to house the lung within the incubator. There are three published lung bioreactors: one that uses Harvard apparatus set-up (Ott et al. 2010), one that uses ventilation only (Price et al. 2010), and one that uses vascular perfusion and a syringe pump to mimic ventilation (Petersen et al. 2010). Ott et al.'s system could be considered the standard for a lung bioreactor, but it is expensive to purchase the unit from Harvard Apparatus. Petersen et al.'s design had a ventilation rate of one breath per minute, which does not fully mimic the physiological respiration rate.

3.5.2 Design

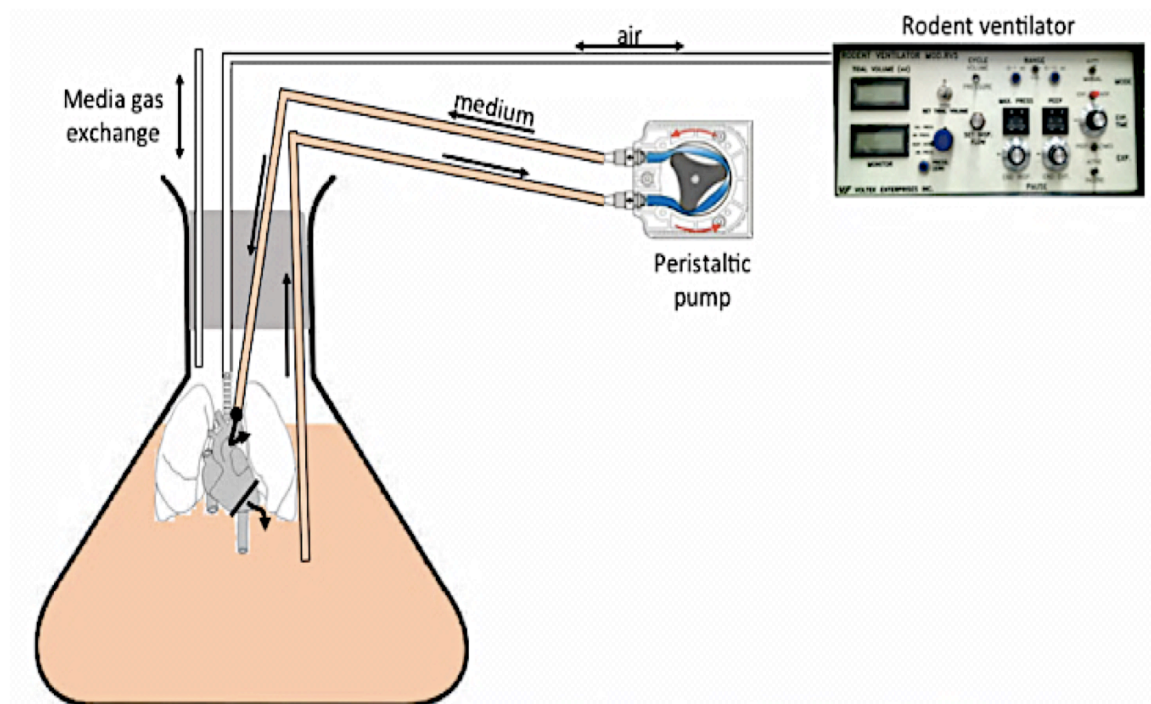


Figure 11-Schematic of lung bioreactor set-up

Housing of the lung bioreactor consisted of a 250 or 125 mL Erlenmeyer flask with an appropriate size rubber stopper with four holes drilled into it. Within these four holes, 1 mL plastic syringes with the ends cut-off were inserted. Plastic tubing was set-up to allow perfusion of lungs and ventilation through these cut-off 1 mL syringes. Trachea and pulmonary artery cannulas were attached to the end of the 1 mL syringe. All components of the bioreactor are autoclavable.

3.5.3 Lung bioreactor culture

Rat lungs that were previously decellularized using the manual whole lung decellularization method and reseeded with cells using the whole lung reseeded method, were cannulated at the pulmonary artery and trachea for culturing. The pulmonary artery cannula was hooked up to a rolling perfusion pump delivering ~250 μL of media per minute. The tracheal cannula was hooked up to a rodent ventilator (model RV5, Voltek Enterprises, Toronto, ON, Canada) and positive ventilation with a pressure of 20 cmH_2O resulting in a breathing rate of ~60 breaths per minute were established. The lung was cultured, perfused, and ventilated in a sterile custom made bioreactor that was housed in a 37°C, 5% CO_2 , 95% O_2 incubator.

3.5.4 Preliminary Results

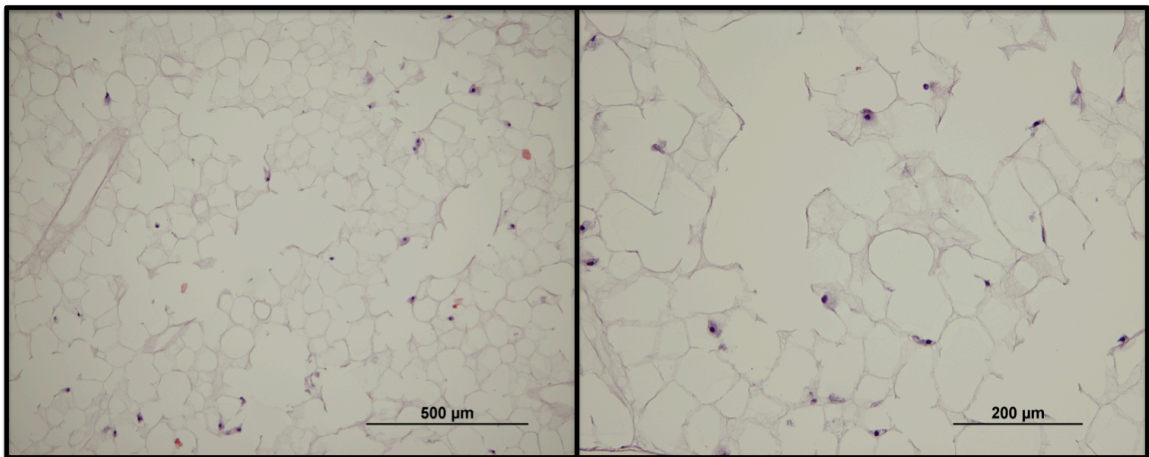


Figure 12-H&E of A549 cells cultured within bioreactor

A549 cells were reseeded onto decellularized lung ECM and cultured within bioreactor for 3 days. H&E demonstrates cells were viable following 3 days of culture.

3.5.5 Discussion

Preliminary results demonstrate that the bioreactor worked and could sustain days long vascular perfusion and physiological respiration. Unfortunately, this thesis did not utilize this technique to evaluate lung ECM-myofibroblast interaction. However, future work could use the bioreactor in tandem with static lung slice culture to better elucidate lung ECM effects on myofibroblast phenotype. Also, the lung bioreactor could be reseeded with many cell types, like stem cells that would study lung regeneration.

3.6 Examination of lung ECM's effects on myofibroblast calcium handling

3.6.1 Background

Since myofibroblasts have increased contractility properties, it would appear logical to examine whether lung ECM could influence fibroblast/myofibroblast Ca^{2+} signaling. Previous studies have revealed two types of myofibroblast contraction: the long isometric contractions regulated by the small GTPase Rho kinase and short ranged contractions controlled by intracellular calcium oscillations (Castella et al. 2010). Previous studies done in our lab and others have shown that fibroblasts and myofibroblasts differ in spontaneous calcium waves and invoked calcium waves when stimulated with growth factors such as TGF- β and PDGF (Castella et al. 2010, Mukherjee et al. 2012, Mukherjee et al. 2013). Moreover, studies have linked the higher contractility in myofibroblasts with greater stiffness from the ECM (Marinković et al. 2012, Balestrini et al. 2012, Trichet et al. 2012).

A study conducted by Godbout et al. (2013) examined the connection between ECM stiffness influences on calcium handling through increased myofibroblast contractility. They found that when ECM stiffness was increased there was a subsequent increase in myofibroblast calcium oscillation. Additionally, they found that myofibroblasts with larger focal adhesions and more developed stress fibers had faster calcium oscillations. One limitation to this study was that they could only modulate stiffness in a 2D environment. In order to fully elucidate lung ECM effects on myofibroblast phenotype, examination of calcium handling as a possible mechanism

through which lung ECM exerts its effect on fibroblast/myofibroblast phenotype could be carried out.

3.6.2 Methods

Whole rat lungs were decellularized using the whole lung decellularization approach using SDC as previously described in the whole lung decellularization method development section. Upon decellularization, whole rat lungs were reseeded with IPF-derived myofibroblasts, and once the agarose hardened the lungs were sectioned into 200 and 300 μm thick slices and cultured in complete RMPI media. Two thicknesses were chosen in order to determine what thickness was optimal for live confocal calcium imaging while maintaining an appropriate 3D microenvironment for cell migration.

Based on previous reseeded results on migration out of agarose onto lung ECM, days 3 and 10 were used for evaluation of spontaneous and overnight TGF- β stimulated myofibroblast calcium handling. Stock solution of Oregon green 488 BAPTA-1 (acetoxymethyl ester) was prepared by dissolving the powdered dye into DMSO and 20% Pluronic acid and stored in small aliquots at $< -20^{\circ}\text{C}$. Prior to imaging, cells plated on glass bottom dishes or reseeded lung slices were incubated in 5 μM of Oregon green 45 mins at 37°C . Confocal microscopy was then performed at room temperature ($21\text{--}23^{\circ}\text{C}$) using a custom-built apparatus based on an inverted Nikon Eclipse TE2000-4 microscope using a 20X objective. To excite Oregon green, a 488-nm illumination from a photodiode laser was scanned across the reseeded lung slice in X- and Y-planes using two oscillating mirrors oscillating at 8 kHz and 30 Hz, respectively. The emitted fluorescence ($>500\text{ nm}$) was detected by a photomultiplier; the signal was then digitized and images generated

(480×400 pixels); recording rate was averaged 10 frames over 1 second. Picture frames were stored as TIF stacks of several hundred frames on a local hard drive using image acquisition software (Video Savant 4.0; IO Industries, London, ON). Image files were then imported into ImageJ (free download: <http://imagej.nih.gov/ij/>).

3.6.3 Preliminary Results

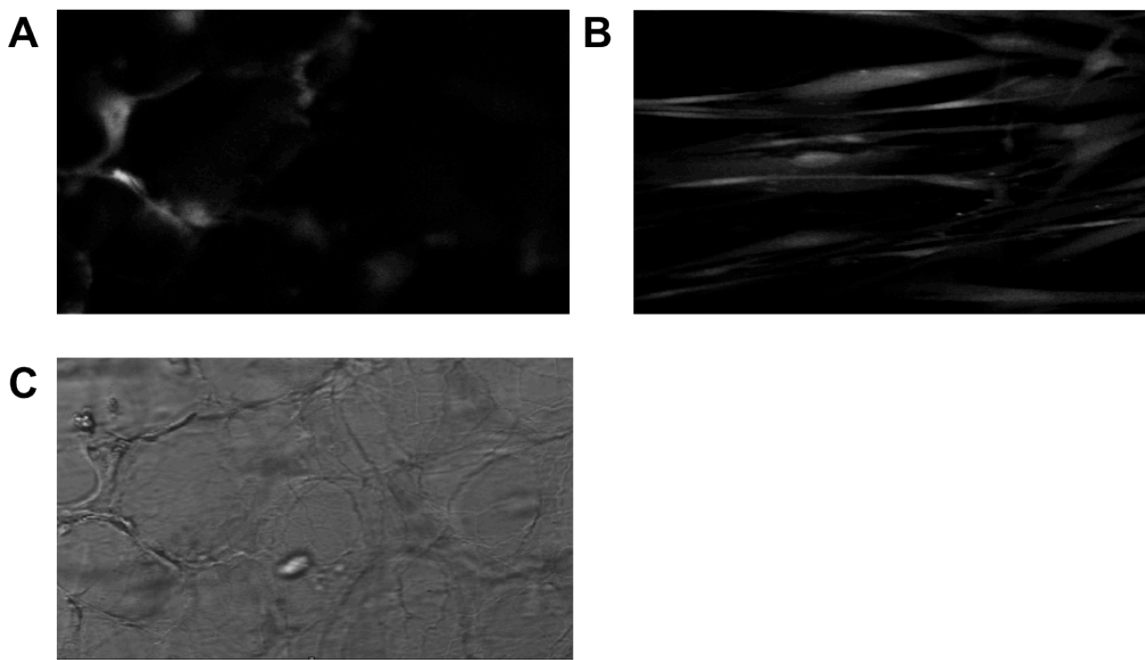


Figure 13-Representation of IPF-derived myofibroblast calcium handling cultured on glass vs. normal lung ECM

A represents IPF-derived myofibroblasts reseeded into whole lung that was sectioned into 200 μm decellularized lung slices loaded with Oregon green to capture calcium activity. B represents same IPF-derived myofibroblasts cultured on glass loaded with Oregon green. C represents the corresponding light image of lung notice the 3D architecture of the lung ECM. Videos were captured at 20X magnification. Utilization of decellularized lung ECM to evaluate myofibroblast calcium handling was successful, and the use of 200

μm thick lung slices was optimal for examining myofibroblast calcium handling with confocal microscopy. Notice the difference in cell size when myofibroblasts were reseeded onto lung ECM compared to culture on glass.

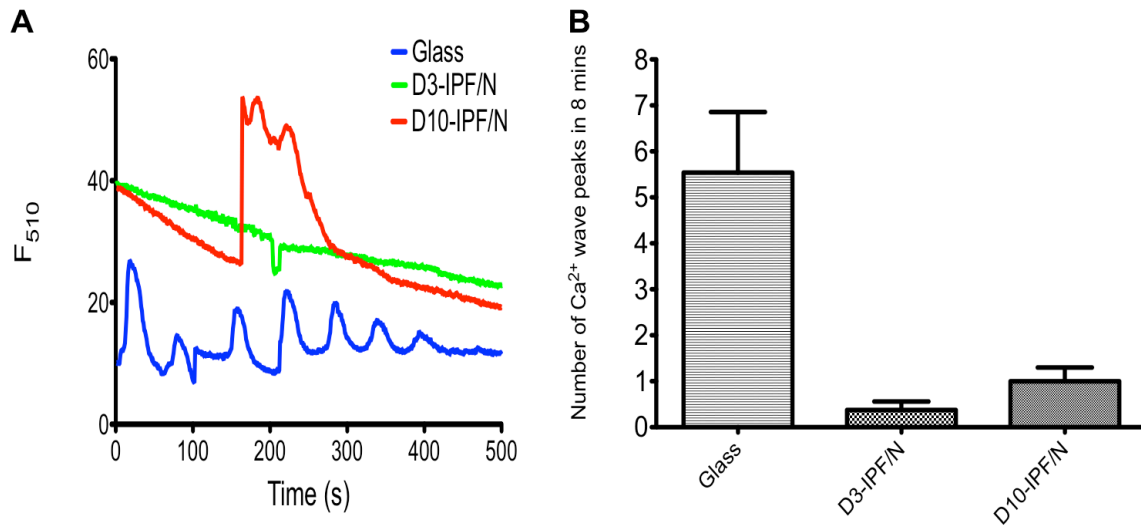


Figure 14-Quantification of normal lung ECM's effect on IPF-derived myofibroblast calcium handling

A represents calcium traces of **B** the average number of calcium peaks when myofibroblasts were cultured on glass or within normal lung ECM for 3 or 10 days. Notice the increase in calcium waves when myofibroblasts were cultured on glass. These results were based on 4 or more cells from the same cell line; therefore, caution should be taken when interpreting this preliminary result.

3.6.3 Discussion

Based on relevant literature search, there were no previous studies examining the effect native lung ECM has on myofibroblast calcium handling. The model developed in this thesis could be an ideal approach in examining lung ECM's effect on fibroblast/myofibroblast calcium handling. Furthermore, future work could compare normal and fibrotic lung ECM and its impacts on fibroblast and myofibroblast phenotype and whether or not calcium handling plays a role in driving any changes.

The increased calcium activity of myofibroblasts cultured on glass compared to the softer lung ECM reflects results from Godbout et al. (2013). The mechanism in which the ECM decreased calcium activity was not examined and it would be convenient to contribute the change in calcium activity based on substrate stiffness. This explanation may prove to be accurate; however, the sequence of events leading to this result needs to be explored. Another explanation could be that there were changes in myofibroblast integrin binding within the normal lung ECM leading to changes in calcium channel activity. Nonetheless, examination of myofibroblast calcium handling in a more physiological 3D environment like the one presented here could help develop novel therapeutic targets for IPF.

Chapter 4: Elucidating Lung ECM Effects on Myofibroblast Phenotype

4.1 Aims

- Determine the phenotype of control and IPF-derived myofibroblasts when cultured on plastic
- Determine whether normal lung ECM could reverse the myofibroblast phenotype
- Attempt to explain the changes induced by normal lung ECM

4.2 Background

Lung fibroblasts have the capability to sense their extracellular environment and are susceptible to differentiation based on increased extracellular matrix stiffening (Tomasek et al. 2002, Grinnell et al. 2003). Traditional cell culture plates have a stiffness in the gigapascal (GPa) range whereas normal lung stiffness ranges from 0.5-3 kPa, which would be a million fold difference (Liu et al. 2010). Previous studies have demonstrated when normal lung was cultured on a stiff cell culture plate it induced fibroblast to myofibroblast differentiation illustrated by an increase in α -SMA expression (Liu et al. 2010, Balestrini et al. 2012, Olsen et al. 2011). The present experiment utilized normal and IPF-derived fibroblast cell lines derived through explantation on plastic.

Balestrini et al. (2012) concluded that explanting a normal lung on a stiff substrate resulted in outgrowth of a myofibroblast population due to overexpression of α -SMA and these myofibroblasts were terminally primed. The term terminally primed refers to the fact that when stiffness induced myofibroblast population was switched to a physiological soft substrate stiffness they did not reverse phenotype. Conversely, when Wang et al. (2012) employed the same experimental design, they found that when valvular

myofibroblasts were switched from a stiff-to-soft substrate there was a reduction in the percent of myofibroblasts noted by a reduction in α -SMA staining. This result was confirmed when explanted pulmonary myofibroblast were switched from stiff-to-soft substrates (Wang et al. 2010). One major limitation of these two studies was that the substrates lacked the three-dimensional architecture of the lung. The present experiments were designed to elucidate a more physiological response by switching myofibroblasts from stiff plastic-to-3D soft, in native lung ECM. Conclusions from this designed experiment would confidently surmise whether myofibroblasts are actually terminally primed. The table below represents the experimental design:

	Control lung explanted on plastic	IPF lung explanted on plastic
Reseeded on Normal lung ECM	Con/N (n=3)	Con/F (n=3)

Control fibroblasts and IPF myofibroblasts were cultured on normal lung ECM for 3 and 10 days, and were subsequently compared to original phenotype gained through culturing on stiff plastic.

4.3 Results

Stiffness of normal and decellularized lungs with and without agarose, as well as the stiffness of the reseeded lung slices used in this experiment was evaluated.

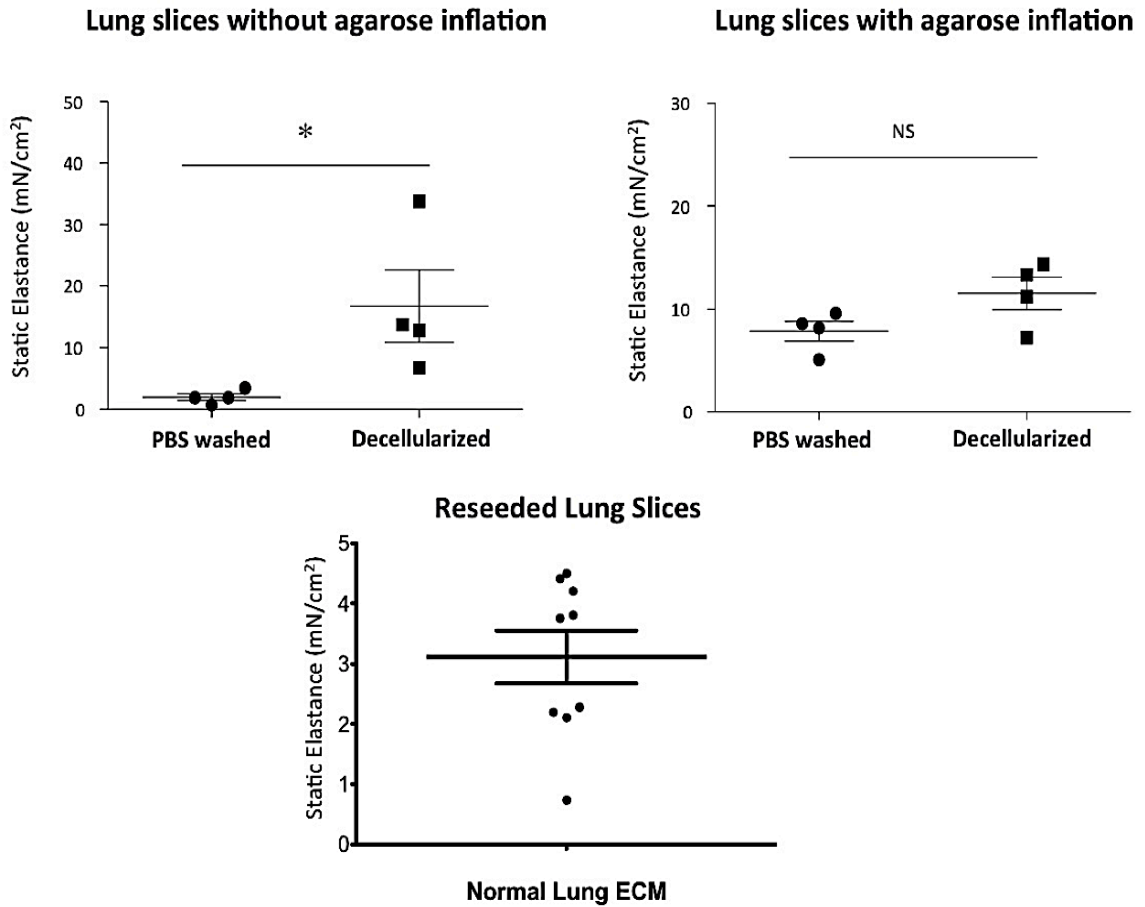


Figure 15-Evaluation of lung slice elastance

Elastance was measured using a custom-built force transducer reading the force one second before and one second after length of the lung slices was increased 0.01 times the resting tissue length. Decellularization increased the stiffness of lungs compared to normal lungs. This difference was normalized when 1% agarose used for reseeding was infused into normal and decellularized lungs. Furthermore, the reseeded lung slices used in the experiments to elucidate lung ECM's effects on fibroblast phenotype reveals that these lung slices were roughly 30 Pa. In comparison to the reported stiffness of plastic was on GPa scale, the reseeded lung slices could be referred to as soft.

An important objective was to determine whether there was a difference in the initial α -SMA expression between control fibroblasts and IPF-derived myofibroblasts following explant and culture on stiff plastic.

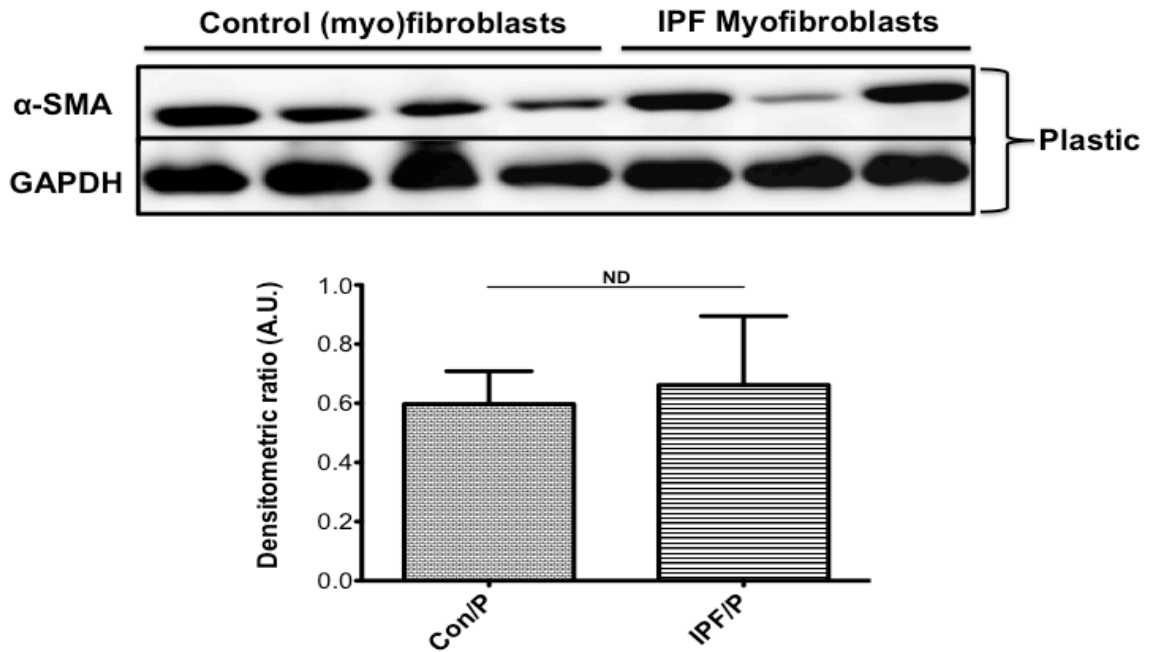


Figure 16-Comparison of control and IPF-derived myofibroblast α -SMA expression when explanted and cultured on plastic

ND stands for no statistical difference. Western blot analysis illustrates that there was no difference in α -SMA expression between control and IPF myofibroblasts, and more importantly that there was high expression of α -SMA in both cell types. With this evidence in hand, the reasoning for designating control fibroblasts as “fibroblasts” instead of myofibroblasts was questioned; it was decided to adopt the terminology of control myofibroblasts instead. Further supporting evidence that control and IPF myofibroblasts had equal α -SMA phenotype was realized in figure 18 where immunocytochemistry for α -SMA was conducted.

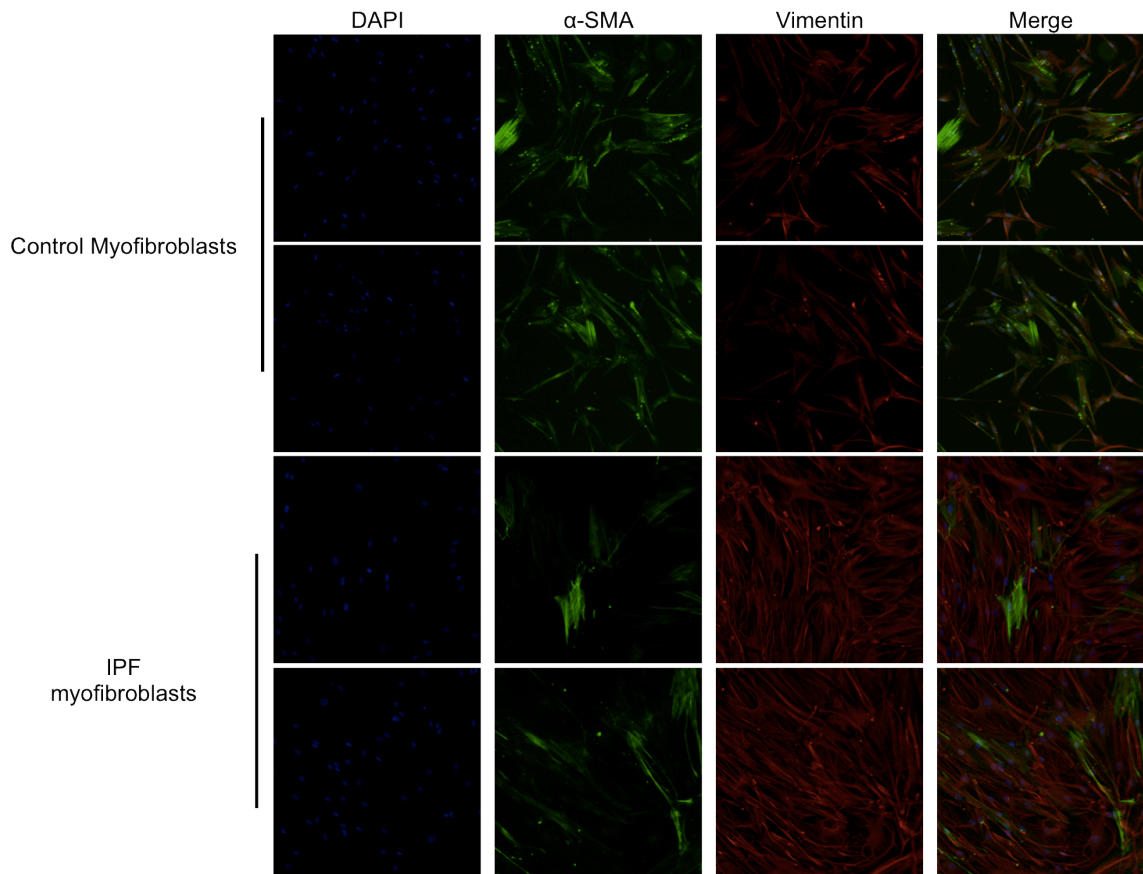


Figure 17-Immunofluorescence of control and IPF-derived myofibroblast α -SMA expression cultured on plastic

DAPI indicates nuclear staining, green indicates myofibroblasts positive for α -SMA, and red indicates myofibroblasts positive for vimentin. Images were taken at 10X magnification.

Figure 17 confirms the result of the previous western blot analysis that both cell types were in fact a majority α -SMA positive myofibroblast population. Additionally, all of the myofibroblasts examined on the slide were vimentin positive indicating that the myofibroblasts were of mesenchymal origin.

Next, α -SMA positive control and IPF myofibroblasts were cultured on decellularized lung ECM in order to determine whether these myofibroblast populations were in fact terminally primed.

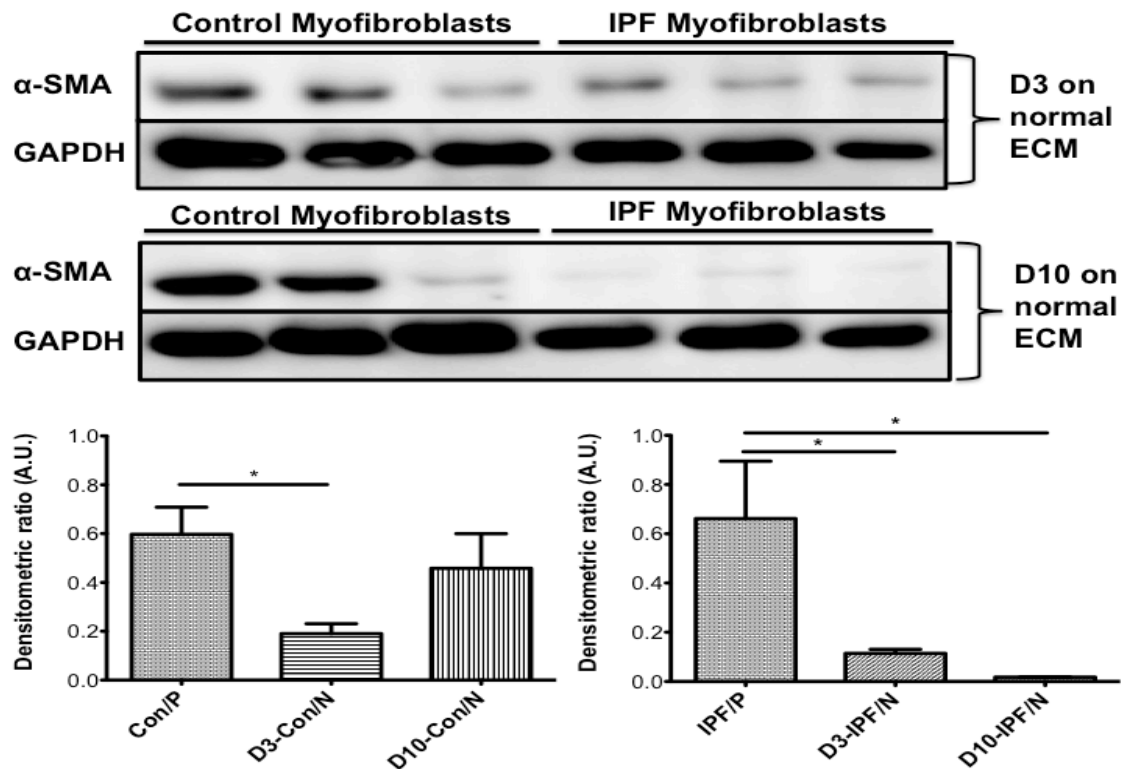


Figure 18-Comparison of control and IPF-derived myofibroblast α -SMA expression following culture on plastic vs. normal lung ECM through western blot analysis

Con=control myofibroblasts, IPF=IPF myofibroblasts, N=Normal lung ECM, D=Day. *

Represents statistical significance $p < 0.05$.

Based on western blot analysis of myfibroblasts reseeded onto normal lung ECM, it was evident that following 3 days of culture on normal lung ECM, control and IPF myfibroblasts experienced a reduction in α -SMA positive expression. Control myfibroblasts α -SMA expression did increase following 10 days of culture; conversely, IPF myfibroblasts experienced a further reduction in α -SMA expression.

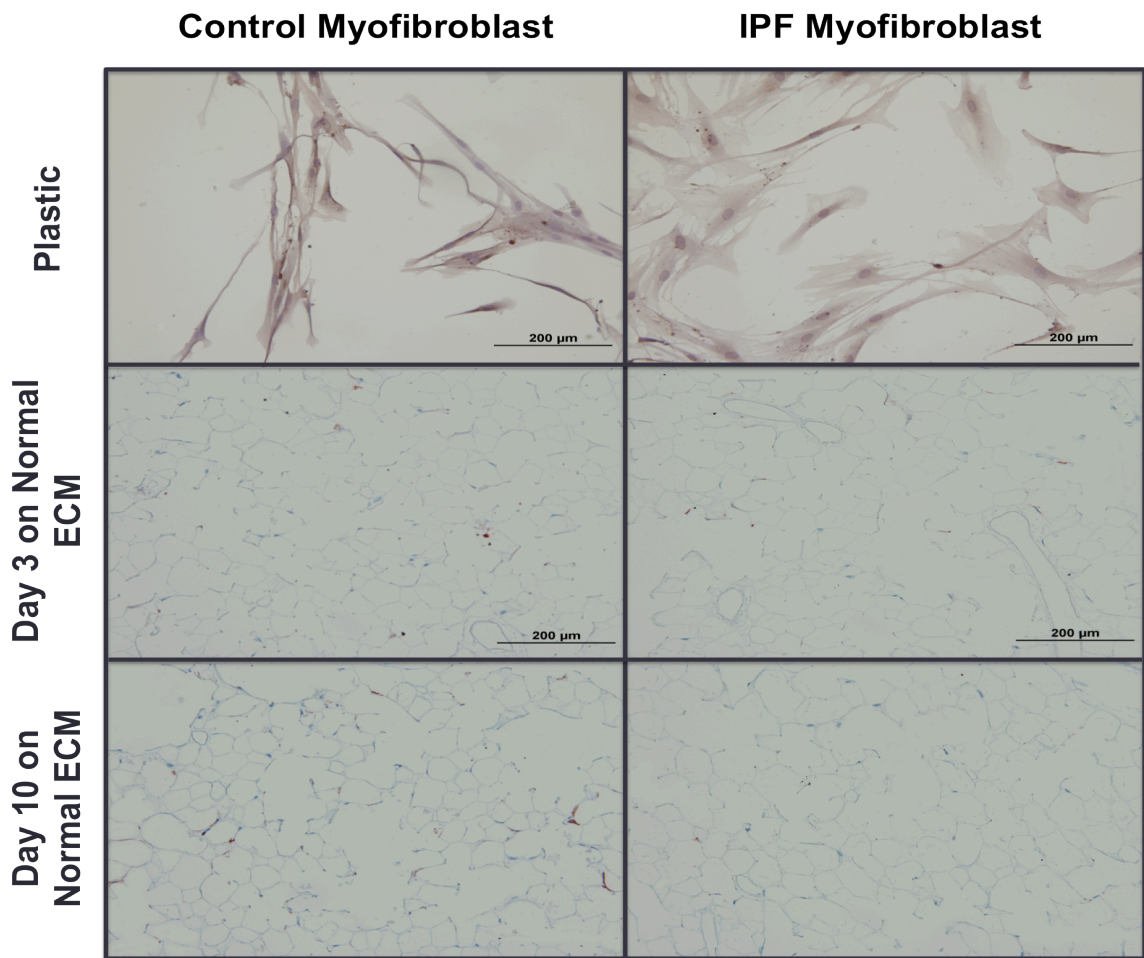


Figure 19-Comparison of control and IPF-derived myfibroblast α -SMA expression following culture on plastic vs. normal lung ECM through immunocytochemistry and immunohistochemistry

Blue stain represents nuclei, light blue represents ECM, and red stain represents α -SMA.

Immunocytochemistry of control and IPF myfibroblasts cultured on plastic confirms the previous immunofluorescence result that the majority of myfibroblasts were α -SMA positive. In comparison, when cultured on softer, normal lung ECM the myfibroblasts were smaller in size and had a reduced α -SMA expression in comparison to culture on plastic. The reduction in α -SMA expression reflects previous western blot analysis.

Since normal lung ECM comprised of both physiological stiffness and native ECM binding domains the question still remained whether or not the change in stiffness, from stiff plastic to normal ECM, reversed the myfibroblast α -SMA expression? To answer this question, control myfibroblasts were cultured on plastic and switched to a 1 kPa soft cell culture plate, which is the physiological stiffness of lung (Liu et al. 2010). The α -SMA expression was then evaluated at days 3 and 10 to match previous results.

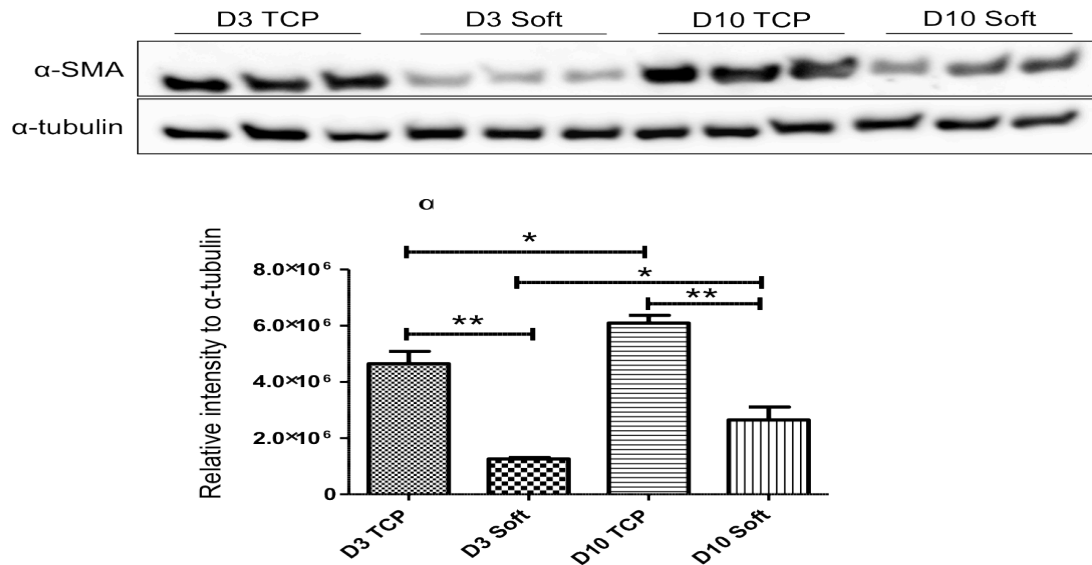


Figure 20-Evaluation of stiff vs. soft cell culture plate effect on control myfibroblast α -SMA expression

TCP=traditional stiff cell culture plastic and soft=1 kPa soft cell culture plate. ** represents statistical significance between TCP and soft culture plate on day 3 or 10 and * represents statistical significance between days 3 and 10.

Western blot analysis in figure 20 (work done by Pierre-Simon Bellaye) revealed that changing the ECM stiffness from stiff to soft was capable of reducing the α -SMA expression in control myofibroblasts at both days 3 and 10. However, changing the ECM stiffness did not abolish the α -SMA expression completely as seen when myofibroblasts were cultured on normal lung ECM.

Next, normal lung ECM effect on myofibroblast apoptosis was evaluated to determine whether or not this was an explanation of the reduction in α -SMA expression. To evaluate this, western blot analysis of caspase-3 and cleaved caspase-3 was carried out.

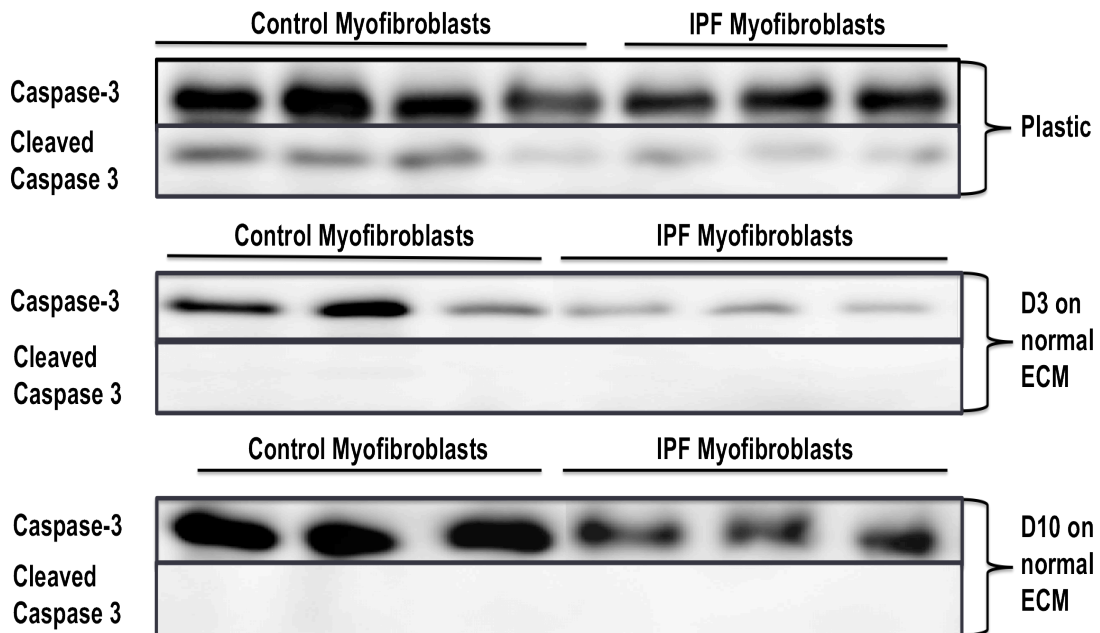


Figure 21-Evaluation of normal lung ECM's effect on myofibroblast apoptosis

Western blot analysis in figure 21 demonstrated that there was a noticeable increase in the active cleaved caspase-3 among control myofibroblasts compared to IPF myofibroblasts cultured on plastic. Interestingly though, there was no detectable cleaved caspase-3 expression among control or IPF myofibroblasts when cultured for 3 or 10 days on normal lung ECM.

4.4 Discussion

One of the major findings from this study would be that both control and IPF myofibroblasts cultured on plastic have identical α -SMA expression. This result was not surprising and was in accordance to previous studies' observations that have clearly shown that culturing fibroblasts on a stiff substrate, like normal tissue culture plates, induced fibroblast to myofibroblast differentiation distinguished by an increase in α -SMA expression (Wipff et al. 2007, Liu et al. 2010, Olsen et al. 2011, Balestrini et al. 2012). Based on the fact that they have indistinguishable α -SMA expression it would lead to the conclusion that they have become identical cell types; however, there could be underlying differences in other myofibroblast characteristics between them that were not tested. More importantly, this result just reinforces the idea that culturing of control and IPF myofibroblasts should reflect respective *in vivo* lung stiffness in order to effectively compare differences. For example, normal lungs should be explanted and cultured on substrates with a stiffness ranging from 0.5-1 kPa reflecting *in vivo* stiffness.

The reduction in α -SMA expression at day 3 for control and IPF myofibroblasts on normal lung ECM and further reduction at day 10 for IPF myofibroblasts indicates that myofibroblasts may not be terminally primed. Furthermore, when control myofibroblasts

were switched from stiff to soft cell culture plates it resulted in a reduction in α -SMA expression as well. This result refutes the notion that myofibroblasts are terminally primed as previously hypothesized by Balestrini et al. (2012). This result aligns with the previous studies' outcomes (Kloxin et al. 2010, Wang et al. 2012) showing that valvular and pulmonary myofibroblasts de-differentiated through a reduction in α -SMA expression when switched from a stiff to soft substrate. Even though there was a reversal in phenotype when myofibroblasts were switched to soft cell culture plates (figure 20), the effect of simply changing substrate stiffness did not fully explain the total reduction in α -SMA expression when cultured on normal lung ECM (figure 18). This result indicates that the change in substrate stiffness may have partially contributed to the decrease in α -SMA expression. However, other mechanisms appear to be involved since there was a further reduction in α -SMA expression when IPF myofibroblasts were cultured on normal lung ECM compared to plastic at day 10 (figure 18, 19, 20).

Booth et al. (2012) cultured normal fibroblasts on normal and fibrotic lung ECM in a similar experimental set-up. Their results indicated that fibrotic ECM was capable of inducing fibroblast to myofibroblast differentiation based on α -SMA expression. Upon further examination of their fibroblast cell culture method revealed that they were culturing their fibroblasts on plastic prior to reseeding onto decellularized lung ECM. Based on evidence presented in this thesis and previous studies, this normal fibroblast culture would have been a majority α -SMA myofibroblast population. Their assumption that they were utilizing normal fibroblasts was most likely flawed; however, their work showed that there was reduction in α -SMA expression following 2 days of culture on

normal lung ECM compared to fibrotic lung ECM. This result suggests that normal ECM had the ability to reverse the myofibroblast phenotype in their study as well. Ultimately, the reduction in α -SMA expression indicated that the initial myofibroblast phenotype transformed into a quiescent-like fibroblast when cultured on normal lung ECM.

There appeared to be an increase in cleaved caspase-3 in control myofibroblasts compared to IPF myofibroblasts demonstrating that there may have been some differences between the two cell lines (figure 21). This result reflects previous work that showed IPF myofibroblasts were protected from apoptosis compared to control fibroblasts (Moodley et al. 2004).

The lack of cleavage of caspase-3 in control and IPF myofibroblasts reseeded on lung ECM at days 3 and 10 when compared to the initial phenotype further suggests that these myofibroblasts de-differentiated into a quiescent fibroblast like state. Alternatively, it could be interpreted that lack of cleaved caspase-3 induced a phenotype that was more resistant to apoptosis. This is an interesting result since Liu et al. (2010) showed that increased stiffness protected against apoptosis and reduced stiffness promoted apoptosis. However, our results indicated that softer lung ECMs have the ability to protect against apoptosis when compared to stiff culture plates. Liu et al. only examined the effect of apoptosis in relation to stiffness, whereas we incorporated both biomechanical (stiffness) and biochemical effects through the use of native lung ECM.

Evidence from Ghaedi et al. (2013) showed that when human induced pluripotent stem cell-derived alveolar type II (iPSC-AETII cells) were cultured on native decellularized lung ECM fewer apoptotic markers were present at days 3 and 7 as

determined by immunostaining for caspase-3. Further evidence suggesting that apoptosis was not in association with a reduction in α -SMA when myofibroblasts were switched from stiff-to-soft substrate was demonstrated by Wang et al. (2012). Furthermore, the reduction in α -SMA expression demonstrated in this thesis was not associated with an increase in apoptosis as well. Nonetheless, in respect to the hypothesis of this thesis, it can be concluded that myofibroblasts adopt the phenotype of the lung ECM they were cultured on as noted by the reversal in α -SMA expression.

4.5 Limitations and Future Directions

Future work utilizing the methods presented in this thesis should help better elucidate lung ECM's effects on fibroblast/myofibroblast phenotype. Recent studies have demonstrated how traditional stiff cell culture plates promote fibroblast to myofibroblast differentiation. With this knowledge in hand, appropriate cell culture conditions should be employed for respective cell types being studied. For example, to study fibrotic lung ECM effects on fibroblast to myofibroblast differentiation, normal lung should be explanted and subcultured on 0.5-1 kPa soft cell culture plates. This stiffness will mimic normal lung tissue elastance and limit the potential for stiffness-induced fibroblast to myofibroblast differentiation.

Utilization of primary human cell lines increases the clinical validity of the experiments carried out in this thesis. Since a large amount of this thesis was methods development, the use of primary human pulmonary myofibroblast cell lines was not ideal. The growth rate and eventual senescence of these cell lines dramatically hampered the rate at which results were obtained. Next steps in the progression of this work may

require further methods refinement, which would benefit from the use of cell lines that can be subcultured past passage 10.

Employment of a xenogenic model of rat lung ECM reseeded with the primary human cell lines may limit the external validity of these results. It would be ideal to decellularize whole human lungs, but acquiring intact human lungs for this purpose would be difficult. One solution would be to use an animal model that more closely resembles human lung physiology like pig or sheep lungs. Ultimately, the *ex vivo* experimental methods developed will never recapitulate *in vivo* conditions, but the methods used in this thesis are more physiological than using traditional plastic cell culture plates used to elucidate differences between normal and IPF myofibroblasts.

The manual decellularization method used in this thesis and other studies used 2% SDC; however, through the rapid decellularization technique, a concentration of 0.5% SDC was equally effective in decellularizing whole rat lung. Therefore, the decellularization with 2% SDC in this thesis may have produced lung ECM that had excess loss in ECM and/or deformation of native ECM conformation. Future work should examine decellularization effects on ECM protein loss through examining insoluble and soluble protein levels with mass spectrometry and deformation of lung ECM through immunofluorescence.

Studying lung ECM effects on myofibroblast phenotype using a static lung slice culture method with agarose does not fully mimic normal lung physiology. The use of agarose within static lung slices could confound results obtained using this method. The use of our novel lung bioreactor mimicking normal lung physiology should be used in

parallel with static lung slice culture in order to confirm the results increasing internal validity of our experiments. The development of the lung bioreactor was a great achievement; however, the reliability of this lung bioreactor has not been fully tested yet. More importantly though, this technique would provide a more accurate model for examining lung ECM effects on fibroblast/myofibroblast phenotype. The lung bioreactor opens up many avenues of exploration like lung regeneration.

Examination of fibrotic lung ECM effects on fibroblast/myofibroblast phenotype was attempted in this thesis. Unfortunately, the administration of TGF- β adenovirus to induce lung pulmonary fibrosis in the rat model produced mild to no fibrosis. In the future, a more effective TGF- β adenovirus concentration should be administered to induce pulmonary fibrosis.

The mechanisms through which normal lung ECM reduced α -SMA expression in myofibroblasts were not fully explained in this thesis. Future work should examine gene and protein expression changes that occurred following myofibroblast reseeding onto normal lung ECM. High throughput screening techniques, like microarray analysis, could develop a conceptual map of the changes that had occurred providing invaluable guidance for future work. Preliminary work examining normal lung ECM effect on myofibroblast calcium handling reveals an interesting avenue for future experimentation as well. Finally, determining whether there were changes in integrin subtype expression may be worth exploring due to integrins role in sensing changes in environmental stiffness and the release of active TGF- β .

References

1. Abe R, Donnelly SC, Peng T, Bucala R, Metz CN. Peripheral blood fibrocytes: Differentiation pathway and migration to wound sites. *J Immunol* 2001;166:7556–62.
2. Andersson-Sjöland A, de Alba CG, Nihlberg K, Becerril C, Ramírez R, Pardo A, Westergren-Thorsson G, Selman M. Fibrocytes are a potential source of lung fibroblasts in idiopathic pulmonary fibrosis. *Int J Biochem Cell Biol* 2008;40:2129–40.
3. American Thoracic Society, European Respiratory Society. American Thoracic Society/European Respiratory Society International Multidisciplinary Consensus Classification of the Idiopathic Interstitial Pneumonias. *Am J Respir Crit Care Med* 2002;165:277–304.
4. Balestrini JL, Chaudhry S, Sarrazy V, Koehler A, Hinz B. The mechanical memory of lung myofibroblasts. *Integr Biol (Camb)* 2012;4:410–21.
5. Barth K, Reh J, Sturrock A, Kasper M. Epithelial vs myofibroblast differentiation in immortal rat lung cell lines—modulating effects of bleomycin. *Histochem Cell Biol* 2005;124:453–64.
6. Bickel M, Baringhaus KH, Gerl M, Günzler V, Kanta J, Schmidts L, Stapf M, Tschank G, Weidmann K, Werner U. Selective inhibition of hepatic collagen accumulation in experimental liver fibrosis in rats by a new prolyl 4-hydroxylase inhibitor. *Hepatology* 1998;28:404–11.

7. Blaauboer ME, Boeijen FR, Emson CL, Turner SM, Zandieh-Doulabi B, Hanemaaijer R, Smit TH, Stoop R, Everts V. Extracellular matrix proteins: A positive feedback loop in lung fibrosis? *Matrix Biol* 2014;34:170–8.
8. Bonvillain RW, Danchuk S, Sullivan DE, Betancourt AM, Semon JA, Eagle ME, Mayeux JP, Gregory AN, Wang G, Townley IK, Borg ZD, Weiss DJ, Bunnell BA. A nonhuman primate model of lung regeneration: detergent-mediated decellularization and initial *in vitro* recellularization with mesenchymal stem cells. *Tissue Eng Pt A* 2012;18:2437–52.
9. Booth AJ, Hadley R, Cornett AM, Dreffs AA, Matthes SA, Tsui JL, Weiss K, Horowitz JC, Fiore VF, Barker TH, Moore BB, Martinez FJ, Niklason LE, White ES. Acellular normal and fibrotic human lung matrices as a culture system for *in vitro* investigation. *Am J Respir Crit Care Med* 2012;186:866–76.
10. Border WA, Noble NA. Transforming growth factor β in tissue fibrosis. *N Engl J Med* 1994;331:1286–92.
11. Braun RK, Martin A, Shah S, Iwashima M, Medina M, Byrne K, Sethupathi P, Wigfield CH, Brand DD, Love RB. Inhibition of bleomycin-induced pulmonary fibrosis through pre-treatment with collagen type V. *J Heart Lung Transplant* 2010;29:873–80.
12. Calle EA, Petersen TH, Niklason LE. Procedure for lung engineering. *J Vis Exp* 2011;49:2651.

13. Castella LF, Buscemi L, Godbout C, Meister JJ, Hinz B. A new lock-step mechanism of matrix remodelling based on subcellular contractile events. *J Cell Sci* 2010;123:1751–60.
14. Castella LF, Gabbiani G, McCulloch CA, Hinz B. Regulation of myofibroblast activities: Calcium pulls some strings behind the scene. *Exp Cell Res* 2010;316:2390–2401.
15. Cavalcante FS, Ito S, Brewer K, Sakai H, Alencar AM, Almeida MP, Andrade JS Jr, Majumdar A, Ingenito EP, Suki B. Mechanical interactions between collagen and proteoglycans: implications for the stability of lung tissue. *J Appl Physiol* 2005;98:672–9.
16. Cox TR, Ertler JT. Remodeling and homeostasis of the extracellular matrix: implications for fibrotic diseases and cancer. *Dis Model Mech* 2011;4:165–78.
17. Daly AB, Wallis JM, Borg ZD, Bonvillain RW, Deng B, Ballif BA, Jaworski DM, Allen GB, Weiss DJ. Initial binding and recellularization of decellularized mouse lung scaffolds with bone marrow-derived mesenchymal stromal cells. *Tissue Eng Pt A* 2012;18:1–16.
18. Decologne N, Kolb M, Margetts PJ, Menetrier F, Artur Y, Garrido C, Gauldie J, Camus P, Bonniaud P. TGF- β 1 induces progressive pleural scarring and subpleural fibrosis. *J Immunol* 2007;179:6043–51.
19. Derynck R, Jarrett JA, Chen EY, Eaton DH, Bell JR, Assoian RK, Roberts AB, Sporn MB, Goeddel DV. Human transforming growth factor- β complementary

- DNA sequence and expression in normal and transformed cells. *Nature* 1985;316:701–5.
20. Desmoulière A, Geinoz A, Gabbiani F, Gabbiani G. Transforming growth factor- β 1 induces α -smooth muscle actin expression in granulation tissue myofibroblasts and in quiescent and growing cultured fibroblasts. *J Cell Biol* 1993;122:103–11.
 21. Desmoulière A, Redard M, Darby I, Gabbiani G. Apoptosis mediates the decrease in cellularity during the transition between granulation tissue and scar. *Am J Pathol* 1995;146:56–66.
 22. Dzamba BJ, Wu H, Jaenisch R, Peters DM. Fibronectin binding site in type I collagen regulates fibronectin fibril formation. *J Cell Biol* 1993;121:1165–72.
 23. Echtermeyer F, Streit M, Wilcox-Adelman S, Saoncella S, Denhez F, Detmar M, Goetinck PF. Delayed wound repair and impaired angiogenesis in mice lacking syndecan-4. *J Clin Invest* 2001;107:R9–R14.
 24. Frid MG, Kale VA, Stenmark KR. Mature vascular endothelium can give rise to smooth muscle cells via endothelial-mesenchymal transdifferentiation: in vitro analysis. *Circ Res* 2002;90:1189–96.
 25. Ghaedi M, Calle EA, Mendez JJ, Gard AL, Balestrini J, Booth A, Bove PF, Gui L, White ES, Niklason LE. Human iPS cell-derived alveolar epithelium repopulates lung extracellular matrix. *J Clin Invest* 2013;123:4950–62.
 26. Gilpin SE, Guyette JP, Gonzalez G, Ren X, Asara JM, Mathisen DJ, Vacanti JP, Ott HC. Perfusion decellularization of human and porcine lungs: Bringing the matrix to clinical scale. *J Heart Lung Transplant* 2014;33:298–308.

27. Godbout C, Castella LF, Smith EA, Talele N, Chow ML, Garonna A, Hinz B. The mechanical environment modulates intracellular calcium oscillation activities of myofibroblasts. *PLoS One* 2013;8:e64560.
28. Goffin JM, Pittet P, Csucs G, Lussi JW, Meister JJ, Hinz B. Focal adhesion size controls tension-dependent recruitment of α -smooth muscle actin to stress fibers. *J Cell Biol* 2006;172:259–68.
29. Grinnell F. Fibroblast biology in three-dimensional collagen matrices. *Trends Cell Biol* 2003;13:264–69.
30. Hashimoto N, Phan SH, Imaizumi K, Matsuo M, Nakashima H, Kawabe T, Shimokata K, Hasegawa Y. Endothelial-mesenchymal transition in bleomycin-induced pulmonary fibrosis. *Am J Respir Cell Mol Biol* 2010;43:161–72.
31. Hedbom E, Heinegård D. Interaction of a 59-kda connective tissue matrix protein with collagen I and collagen II. *J Biol Chem* 1989;264:6898–905.
32. Henderson NC, Arnold TD, Katamura Y, Giacomini MM, Rodriguez JD, McCarty JH, Pellicoro A, Raschperger E, Betsholtz C, Ruminski PG, Griggs DW, Prinsen MJ, Maher JJ, Iredale JP, Lacy-Hulbert A, Adams RH, Sheppard D. Targeting of α v integrin depletion identifies a core, targetable molecular pathway that regulates fibrosis across solid organs. *Nat Med* 2013;19:1617-24.
33. Hernnäs J, Nettelbladt O, Bjermer L, Särnstrand B, Malmström A, Hällgren R. Alveolar accumulation of fibronectin and hyaluronan precedes bleomycin-induced pulmonary fibrosis in the rat. *Eur Respir J* 1992;5:404–10.

34. Hinz B, Celetta G, Tomasek JJ, Gabbiani G, Chaponnier C. Alpha-smooth muscle actin expression upregulates fibroblast contractile activity. *Mol Biol Cell* 2001;12:2730–41.
35. Hinz B. Masters and servants of the force: The role of matrix adhesions in myofibroblast force perception and transmission. *Eur J Cell Biol* 2006;85:175–81.
36. Hinz B, Gabbiani G, Chaponnier C. The NH₂-terminal peptide of α -smooth muscle actin inhibits force generation by the myofibroblast in vitro and in vivo. *J Cell Biol* 2002;157:657–63.
37. Hinz B, Phan SH, Thannickal VJ, Galli A, Bochaton-Piallat ML, Gabbiani G. The myofibroblast: one function, multiple origins. *Am J Pathol* 2007;170:1807–16.
38. Hubbard R, Johnston I, Britton J. Survival in patients with cryptogenic fibrosing alveolitis. *Chest* 1998;113:396–400.
39. Humphreys BD, Lin SL, Kobayashi A, Hudson TE, Nowlin BT, Bonventre JV, Valerius MT, McMahon AP, Duffield JS. Fate tracing reveals the pericyte and not epithelial origin of myofibroblasts in kidney fibrosis. *Am J Pathol* 2010;176:85–97.
40. Hutchison N, Fligny C, Duffield JS. Resident mesenchymal cells and fibrosis. *Biochim Biophys Acta* 2013;1832:962–71.
41. Hynes RO. The extracellular matrix: not just pretty fibrils. *Science* 2009;326:1216–9.
42. Iozzo RV. Matrix proteoglycans: from molecular design to cellular function. *Annu Rev Biochem* 1998;67:609–52.

43. Iozzo V, Murdoch AD. Proteoglycans of the extracellular environment: clues from the gene and protein side offer novel perspectives in molecular diversity and function. *FASEB J* 1996;10:598–614.
44. Jenkins G. The role of proteases in transforming growth factor- β activation. *Int J Biochem Cell Biol* 2008;40:1068–78.
45. Jensen T, Roszell B, Zang F, Girard E, Matson A, Thrall R, Jaworski DM, Hatton C, Weiss DJ, Finck C. A rapid lung de-cellularization protocol supports embryonic stem cell differentiation *in vitro* and following implantation. *Tissue Eng Pt C Meth* 2012;18:632–46.
46. Kagan HM, Trackman PC. Properties and function of lysyl oxidase. *Am J Respir Cell Mol Biol* 1991;5:206–10.
47. Kalluri R, Neilson EG. Epithelial-mesenchymal transition and its implications for fibrosis. *J Clin Invest* 2003;112:1776–84.
48. Kim KK, Kugler MC, Wolters PJ, Robillard L, Galvez MG, Brumwell AN, Sheppard D, Chapman HA. Alveolar epithelial cell mesenchymal transition develops *in vivo* during pulmonary fibrosis and is regulated by the extracellular matrix. *Proc Natl Acad Sci U S A* 2006;103:13180–5.
49. King TE Jr, Schwarz MI, Brown K, Tooze JA, Colby TV, Waldron JA Jr, Flint A, Thurlbeck W, Cherniack RM. Idiopathic pulmonary fibrosis: Relationship between histopathologic features and mortality. *Am J Respir Crit Care Med* 2001;164:1025–32.

50. Klass CM, Couchman JR, Woods A. Control of extracellular matrix assembly by syndecan-2 proteoglycan. *J Cell Sci* 2000;113:493–506.
51. Kloxin AM, Benton JA, Anseth KS. *In situ* elasticity modulation with dynamic substrates to direct cell phenotype. *Biomaterials* 2010;31:1–8.
52. Kohan M, Muro AF, White ES, Berkman N. EDA-containing cellular fibronectin induces fibroblast differentiation through binding to $\alpha_4\beta_7$ integrin receptor and MAPK/Erk 1/2-dependent signaling. *FASEB J* 2010;24:4503–12.
53. Kolb M, Margetts PJ, Anthony DC, Pitossi F, Gauldie J. Transient expression of IL-1 β induces acute lung injury and chronic repair leading to pulmonary fibrosis. *J Clin Invest* 2001;107:1529–36.
54. Liu F, Mih JD, Shea BS, Kho AT, Sharif AS, Tager AM, Tschumperlin DJ. Feedback amplification of fibrosis through matrix stiffening and COX-2 suppression. *J Cell Biol* 2010;190:693–706.
55. Maher TM, Evans IC, Bottoms SE, Mercer PF, Thorley AJ, Nicholson AG, Laurent GJ, Tetley TD, Chambers RC, McAnulty RJ. Diminished prostaglandin E2 contributes to the apoptosis paradox in idiopathic pulmonary fibrosis. *Am J Respir Crit Care Med* 2010;182:73–82.
56. Margetts PJ, Bonniaud P, Liu L, Hoff CM, Holmes CJ, West-Mays JA, Kelly MM. Transient overexpression of TGF- β 1 induces epithelial mesenchymal transition in the rodent peritoneum. *J Am Soc Nephrol* 2005;16:425–36.
57. Marinković A, Mih JD, Park JA, Liu F, Tschumperlin DJ. Improved throughput traction microscopy reveals pivotal role for matrix stiffness in fibroblast

- contractility and TGF- β responsiveness. *Am J Physiol Lung Cell Mol Physiol* 2012;303:L169–80.
58. Masszi A, Di Ciano C, Sirokmány G, Arthur WT, Rotstein OD, Wang J, McCulloch CA, Rosivall L, Mucsi I, Kapus A. Central role for Rho in TGF- β 1-induced α -smooth muscle actin expression during epithelial-mesenchymal transition. *Am J Physiol Renal Physiol* 2003;284:F911–24.
59. Midwood KS, Valenick LV, Hsia HC, Schwarzbauer JE. Coregulation of fibronectin signaling and matrix contraction by tenascin-c and syndecan-4. *Mol Biol Cell* 2004;15:5670–7.
60. Moeller A, Gilpin SE, Ask K, Cox G, Cook D, Gauldie J, Margetts PJ, Farkas L, Dobranowski J, Boylan C, O’Byrne PM, Strieter RM, Kolb M. Circulating fibrocytes are an indicator of poor prognosis in idiopathic pulmonary fibrosis. *Am J Respir Crit Care Med* 2009;179:588–94.
61. Moodley YP, Caterina P, Scaffidi AK, Misso NL, Papadimitriou JM, McAnulty RJ, Laurent GJ, Thompson PJ, Knight DA. Comparison of the morphological and biochemical changes in normal human lung fibroblasts and fibroblasts derived from lungs of patients with idiopathic pulmonary fibrosis during FasL-induced apoptosis. *J Pathol* 2004;202:486–95.
62. Mukherjee S, Duan F, Kolb MR, Janssen LJ. Platelet derived growth factor-evoked Ca²⁺ wave and matrix gene expression through phospholipase C in human pulmonary fibroblast. *Int J Biochem Cell Biol* 2013;45:1516–24.

63. Mukherjee S, Kolb MR, Duan F, Janssen LJ. Transforming growth factor- β evokes ca^{2+} waves and enhances gene expression in human pulmonary fibroblasts. *Am J Respir Cell Mol Biol* 2012;46:757–64.
64. Munger JS, Huang X, Kawakatsu H, Griffiths MJ, Dalton SL, Wu J, Pittet JF, Kaminski N, Garat C, Matthay MA, Rifkin DB, Sheppard D. The integrin $\alpha v \beta 6$ binds and activates latent TGF β 1: a mechanism for regulating pulmonary inflammation and fibrosis. *Cell* 1999;96:319–28.
65. Muro AF, Chauhan AK, Gajovic S, Iaconcig A, Porro F, Stanta G, Baralle FE. Regulated splicing of the fibronectin EDA exon is essential for proper skin wound healing and normal lifespan. *J Cell Biol* 2003;162:149–60.
66. Muro AF, Moretti FA, Moore BB, Yan M, Atrasz RG, Wilke CA, Flaherty KR, Martinez FJ, Tsui JL, Sheppard D, Baralle FE, Toews GB, White ES. An essential role for fibronectin extra type iii domain a in pulmonary fibrosis. *Am J Respir Crit Care Med* 2008;177:638–45.
67. Nettelblatt O, Hällgren R. Hyaluronan (hyaluronic acid) in Bronchoalveolar Lavage Fluid during the Development of Bleomycin-induced Alveolitis in the Rat. *Am Rev Respir Dis* 1989;140:1028–32.
68. Olsen AL, Bloomer SA, Chan EP, Gaça MD, Georges PC, Sackey B, Uemura M, Janmey PA, Wells RG. Hepatic stellate cells require a stiff environment for myofibroblastic differentiation. *Am J Physiol Gastrointest Liver Physiol* 2011;301:G110–8.

69. Olsen KC, Sapinoro RE, Kottmann RM, Kulkarni AA, Iismaa SE, Johnson GV, Thatcher TH, Phipps RP, Sime PJ. Transglutaminase 2 and its role in pulmonary fibrosis. *Am J Respir Crit Care Med* 2011;184:699–707.
70. Ott HC, Clippinger B, Conrad C, Schuetz C, Pomerantseva I, Ikonomidou L, Kotton D, Vacanti JP. Regeneration and orthotopic transplantation of a bioartificial lung. *Nat Med* 2010;16:927–33.
71. Papakonstantinou E, Karakioulakis G. The ‘sweet’ and ‘bitter’ involvement of glycosaminoglycans in lung diseases: pharmacotherapeutic relevance. *Br J Pharmacol* 2009;157:1111–27.
72. Petersen TH, Calle EA, Zhao L, Lee EJ, Gui L, Raredon MB, Gavrillov K, Yi T, Zhuang ZW, Breuer C, Herzog E, Niklason LE. Tissue-engineered lungs for in vivo implantation. *Science* 2010;329:538–41.
73. Phillips RJ, Burdick MD, Hong K, Lutz MA, Murray LA, Xue YY, Belperio JA, Keane MP, Strieter RM. Circulating fibrocytes traffic to the lungs in response to CXCL12 and mediate fibrosis. *J Clin Invest* 2004;114: 438-46.
74. Pociask DA, Sime PJ, Brody AR. Asbestos-derived reactive oxygen species activate TGF- β 1. *Lab Invest* 2004;84:1013–23.
75. Poletti V, Ravaglia C, Buccioli M, Tantalocco P, Piciocchi S, Dubini A, Carloni A, Chilosi M, Tomassetti S. Idiopathic pulmonary fibrosis: diagnosis and prognostic evaluation. *Respiration* 2013;86:5–12.
76. Pöschl E, Schlötzer-Schrehardt U, Brachvogel B, Saito K, Ninomiya Y, Mayer U. Collagen IV is essential for basement membrane stability but dispensable for

- initiation of its assembly during early development. *Development* 2004;131:1619–28.
77. Price AP, England KA, Matson AM, Blazar BR, Panoskaltsis-Mortari A. Development of a Decellularized Lung Bioreactor System for Bioengineering the Lung: The Matrix Reloaded. *Tissue Eng Pt A* 2010;16:2581–91.
78. Raghu G, Collard HR, Egan JJ, Martinez FJ, Behr J, Brown KK, Colby TV, Cordier J-F, Flaherty KR, Lasky JA, Lynch DA, Ryu JH, Swigris JJ, Wells AU, Ancochea J, Bouros D, Carvalho C, Costabel U, Ebina M, Hansell DM, Johkoh T, Kim DS, King TE Jr., Kondoh Y, Myers J, Müller NL, Nicholson AG, Richeldi L, Selman M, Dudden RF, Griss BS, Protzko SL, Schönemann HJ. An official ATS/ERS/JRS/ALAT statement: Idiopathic pulmonary fibrosis: Evidence-based guidelines for diagnosis and management. *Am J Respir Crit Care Med* 2011;183:788–824.
79. Raghu G, Weycker D, Edelsberg J, Bradford WZ, Oster G. Incidence and prevalence of idiopathic pulmonary fibrosis. *Am J Respir Crit Care Med* 2006;174:810–6.
80. Ramos C, Montañó M, García-Alvarez J, Ruiz V, Uhal BD, Selman M, Pardo A. Fibroblasts from idiopathic pulmonary fibrosis and normal lungs differ in growth rate, apoptosis, and tissue inhibitor of metalloproteinases expression. *Am J Respir Cell Mol Biol* 2001;24:591–8.
81. Reed CC, Iozzo RV. The role of decorin in collagen fibrillogenesis and skin homeostasis. *Glycoconj J* 2002;19:249–55.

82. Reiser K, McCormick RJ, Rucker RB. Enzymatic and nonenzymatic cross-linking of colagen and elastin. *FASEB J* 1992;6:2439–49.
83. Richeldi L, du Bois RM, Raghu G, Azuma A, Brown KK, Costabel U, Cottin V, Flaherty KR, Hansell DM, Inoue Y, Kim DS, Kolb M, Nicholson AG, Noble PW, Selman M, Taniguchi H, Brun M, Le Maulf F, Girard M, Stowasser S, Schlenker-Herceg R, Disse B, Collard HR. Efficacy and safety of nintedanib in idiopathic pulmonary fibrosis. *N Engl J Med* 2014;370:2071–82.
84. Rocco PR, Negri EM, Kurtz PM, Vasconcellos FP, Silva GH, Capelozzi VL, Romero PV, Zin WA. Lung tissue mechanics and extracellular matrix remodeling in acute lung injury. *Am J Respir Crit Care Med* 2001;164:1067–71.
85. Rock JR, Barkauskas CE, Cronic MJ, Xue Y, Harris JR, Liang J, Noble PW, Hogan BL. Multiple stromal populations contribute to pulmonary fibrosis without evidence for epithelial to mesenchymal transition. *Proc Natl Acad Sci U S A* 2011;108:E1475–83.
86. Ruoslahti E, Yamaguchi Y. Proteoglycans as modulators of growth factor activities. *Cell* 1991;64:867-9.
87. San Antonio JD, Lander AD, Karnovsky MJ, Slayter HS. Mapping the heparin-binding sites on type I collagen monomers and fibrils. *J Cell Biol* 1994;125:1179–88.
88. Sand JM, Larsen L, Hogaboam C, Martinez F, Han M, Røssel Larsen M, Nawrocki A, Zheng Q, Karsdal MA, Leeming DJ. MMP mediated degradation of type IV collagen alpha 1 and alpha 3 chains reflects basement membrane

- remodeling in experimental and clinical fibrosis--validation of two novel biomarker assays. *PLoS One* 2013;8:e84934.
89. Scarritt ME, Bonvillain RW, Burkett BJ, Wang G, Glotser EY, Zhang Q, Sammarco MC, Betancourt AM, Sullivan DE, Bunnell BA. Hypertensive rat lungs retain hallmarks of vascular disease upon decellularization but support the growth of mesenchymal stem cells. *Tissue Eng Pt A* 2014;20:1426–43.
90. Schürch W, Seemayer T, Gabbiani G. the myofibroblast: a quarter century after its discovery back to top. *Am J Surg Pathol* 1998;22:141–7.
91. Serini G, Bochaton-Piallat ML, Ropraz P, Geinoz A, Borsi L, Zardi L, Gabbiani G. The fibronectin domain ED-A is crucial for myofibroblastic phenotype induction by transforming growth factor- β 1. *J Cell Biol* 1998;142:873–81.
92. Sime PJ, Xing Z, Graham FL, Csaky KG, Gauldie J. Adenovector-mediated gene transfer of active transforming growth factor- β 1 induces prolonged severe fibrosis in rat lung. *J Clin Invest* 1997;100:768–76.
93. Souza-Fernandes AB, Pelosi P, Rocco PR. Bench-to-bedside review: The role of glycosaminoglycans in respiratory disease. *Crit Care* 2006;10:237.
94. Sullivan DE, Ferris M, Pociask D, Brody AR. The latent form of $\text{tgf}\beta$ 1 is induced by $\text{tnf}\alpha$ through an erk specific pathway and is activated by asbestos-derived reactive oxygen species *in vitro* and *in vivo*. *J Immunotoxicol* 2008;5:145–9.
95. Tomasek JJ, Gabbiani G, Hinz B, Chaponnier C, Brown RA. Myofibroblasts and mechano-regulation of connective tissue remodelling. *Nat Rev Mol Cell Biol* 2002;3:349–63.

96. Trichet L, Le Digabel J, Hawkins RJ, Vedula SR, Gupta M, Ribault C, Hersen P, Voituriez R, Ladoux B. Evidence of a large-scale mechanosensing mechanism for cellular adaptation to substrate stiffness. *Proc Natl Acad Sci U S A* 2012;109:6933–8.
97. Tumova S, Woods A, Couchman JR. Heparan sulfate proteoglycans on the cell surface: versatile coordinators of cellular functions. *Int J Biochem Cell Biol* 2000;32:269–88.
98. Van Hoozen BE, Grimmer KL, Marelich GP, Armstrong LC, Last JA. Early phase collagen synthesis in lungs of rats exposed to bleomycin. *Toxicology* 2000;147:1–13.
99. Vaughan MB, Howard EW, Tomasek JJ. Transforming growth factor- β 1 promotes the morphological and functional differentiation of the myofibroblast. *Exp Cell Res* 2000;257:180–9.
100. Venkatesan N, Ouzzine M, Kolb M, Netter P, Ludwig MS. Increased deposition of chondroitin/dermatan sulfate glycosaminoglycan and upregulation of β 1,3-glucuronosyltransferase I in pulmonary fibrosis. *Am J Physiol Lung Cell Mol Physiol* 2011;300:L191–L203.
101. Villena J, Berndt C, Granés F, Reina M, Vilaró S. Syndecan-2 expression enhances adhesion and proliferation of stably transfected Swiss 3T3 cells. *Cell Biol Int* 2003;27:1005–10.

102. Wakefield LM, Smith DM, Flanders KC, Sporn MB. Latent transforming growth factor- β from human platelets. A high molecular weight complex containing precursor sequences. *J Biol Chem* 1988;263:7646–54.
103. Wallis JM, Borg ZD, Daly AB, Deng B, Ballif BA, Allen GB, Jaworski DM, Weiss DJ. Comparative assessment of detergent-based protocols for mouse lung de-cellularization and re-cellularization. *Tissue Eng Pt C Meth* 2012;18:420–432.
104. Wang H, Haeger SM, Kloxin AM, Leinwand LA, Anseth KS. Redirecting valvular myofibroblasts into dormant fibroblasts through light-mediated reduction in substrate modulus. *PLoS One* 2012;7:e39969.
105. Willis BC, duBois RM, Borok Z. Epithelial origin of myofibroblasts during fibrosis in the lung. *Proc Am Thorac Soc* 2006;3:377–82.
106. Willis BC, Liebler JM, Luby-Phelps K, Nicholson AG, Crandall ED, du Bois RM, Borok Z. Induction of epithelial-mesenchymal transition in alveolar epithelial cells by transforming growth factor- β 1: potential role in idiopathic pulmonary fibrosis. *Am J Pathol* 2005;166:1321–32.
107. Wipff PJ, Rifkin DB, Meister JJ, Hinz B. Myofibroblast contraction activates latent TGF- β 1 from the extracellular matrix. *J Cell Biol* 2007;179:1311–23.
108. Yokota T, Kawakami Y, Nagai Y, Ma JX, Tsai JY, Kincade PW, Sato S. Bone marrow lacks a transplantable progenitor for smooth muscle type alpha-actin-expressing cells. *Stem Cells* 2006;24:13–22.
109. Yurchenco PD, Schittny JC. Molecular architecture of basement membranes. *FASEB J* 1990;4:1577-90.

110. Zavadil J, Böttinger EP. TGF- β and epithelial-to-mesenchymal transitions. *Oncogene* 2005;24:5764–74.
111. Zhang K, Rekhter MD, Gordon D, Phan SH. Myofibroblasts and their role in lung collagen gene expression during pulmonary fibrosis. A combined immunohistochemical and in situ hybridization study. *Am J Pathol* 1994;145:114–25.
112. Zhou Z, Wang J, Cao R, Morita H, Soininen R, Chan KM, Liu B, Cao Y, Tryggvason K. Impaired angiogenesis, delayed wound healing and retarded tumor growth in perlecan heparan sulfate-deficient mice. *Cancer Res* 2004;64:4699–702.